water

MDPI

Review

Advances and Challenges in Adsorbent Materials for Rainwater Treatment

Gabriela T. A. D. Santos, Armando C. Duarte and Patrícia S. M. Santos *

CESAM & Department of Chemistry, University of Aveiro, Campus Universitário de Santiago, 3810-193 Aveiro, Portugal; gtads@ua.pt (G.T.A.D.S.); aduarte@ua.pt (A.C.D.)
* Correspondence: patricia.santos@ua.pt

Abstract

Rainwater harvesting is increasingly recognized as a sustainable supplement to conventional water supplies and a strategy to improve water resilience. However, harvested rainwater may contain organic and inorganic contaminants introduced by atmospheric deposition and contact with collection surfaces, requiring adequate treatment before safe use. This review critically evaluates the application of adsorbent materials for harvested rainwater treatment, namely carbon-based materials, surface-modified mineral matrices, and biosorbents. The available literature was analyzed considering adsorbent characteristics, treatment conditions, removal performance, and the mechanisms potentially governing contaminant removal. The reviewed studies demonstrate that activated carbon is the most investigated adsorbent class, while surface-modified minerals and biosorbents remain less explored. Direct comparison between studies is limited by differences in experimental conditions and incomplete characterization of adsorbent properties. Adsorption performance depends on both adsorbent characteristics and rainwater chemistry, particularly pH, which affects surface charge and the aqueous speciation of many contaminants. Reported removal efficiencies do not always reflect adsorption alone, as treatment configuration and operating conditions may also promote precipitation, physical retention, and in some cases, biologically mediated degradation. Future research should prioritize standardized material characterization, mechanistic evaluation, regeneration strategies, and long-term validation to support the development of more predictable and reproducible rainwater treatment technologies.

Keywords: adsorbents; activated carbon; coated sand; biosorbent; rainwater treatment; organic and inorganic contaminants

Check for updates

Academic Editor: Laura Bulgariu

Received: 15 July 2026
Revised: 29 July 2026
Accepted: 3 August 2026
Published: 10 August 2026

Copyright: © 2026 by the authors. Licensee MDPI, Basel, Switzerland. This article is an open access article distributed under the terms and conditions of the Creative Commons Attribution (CC BY) license.

1. Introduction

Freshwater scarcity has become one of the major challenges for sustainable water management because of population growth, rapid urbanization, industrial development, and climate change [1]. According to the Sixth Assessment Report of the Intergovernmental Panel on Climate Change (IPCC AR6), climate change is expected to intensify water scarcity and water stress while increasing the frequency of both drought and extreme precipitation events in many regions of the world [2]. These changes highlight the need for adaptation strategies capable of diversifying water resources and strengthening the resilience of urban water systems. Within this context, rainwater harvesting has emerged as a decentralized approach that can supplement conventional water supplies, reduce pressure on freshwater resources, and contribute to more climate-resilient cities. Although rainwater harvesting

represents a promising alternative water resource, the quality of harvested rainwater largely determines its suitability for different applications and the level of treatment required to achieve the quality requirements of the intended application.

Rainwater is an atmospheric aqueous phase whose chemical composition results from continuous interactions with gaseous species, aerosols, and particulate matter during cloud formation and subsequent precipitation [3,4]. Such interactions promote the incorporation of inorganic ions, metals, organic compounds, and secondary products formed through photochemical and oxidative pathways [5–7]. Therefore, rainwater constitutes a chemically dynamic matrix whose composition is strongly influenced by local emission sources, long-range atmospheric transport and environmental conditions. Rainwater may contain complex mixtures of major ions, potentially toxic elements [8], and dissolved organic matter (DOM) [9], with concentrations that vary significantly across locations and precipitation events, thereby affecting its quality and suitability for different applications. Under certain conditions, these constituents may reach concentrations associated with risks to human health and ecosystem integrity, e.g., [10,11]. The level of treatment required depends on both the intended application and the chemical composition of the harvested rainwater. Therefore, rainwater treatment is not intended for the remediation of all precipitation at a regional scale, but rather for improving the quality of harvested rainwater stored for specific applications where higher water quality requirements apply, including domestic non-potable uses, irrigation, and other decentralized water supply purposes.

Adsorption has attracted considerable attention for rainwater treatment because it relies on surface-mediated interactions that enable the removal of a wide range of dissolved contaminants. Its effectiveness is determined by the physicochemical properties of the adsorbent, including surface chemistry, functional groups, and porosity [12,13]. In this context, the selection of adsorbent material becomes a key factor governing removal efficiency and selectivity [14], particularly considering the inherent chemical variability of harvested rainwater. A range of adsorbent materials has been investigated for rainwater treatment, including carbon-based materials, surface-modified mineral matrices, and biosorbents, e.g., [15–17]. These adsorbents exhibit distinct structural and chemical features, which influence their performance under different rainwater conditions and contaminant profiles.

Despite the expanding literature on this topic, studies are typically conducted under different experimental conditions and tend to focus on specific materials or target contaminants, limiting meaningful comparisons across material classes. Moreover, a variety of approaches have been investigated, including systems that operate based exclusively on adsorbent materials and hybrid or multi-step configurations combining different processes. This lack of standardization results in fragmented understanding of how adsorbent properties translate into performance under realistic rainwater conditions. In particular, the relationship between material structure, surface chemistry, and multi-contaminant removal remains insufficiently integrated across the literature.

To the best of our knowledge, this is the first review to critically examine adsorbent materials applied to real rainwater samples. It focuses on carbon-based materials, surface-modified mineral matrices, and biosorbents, relating their structural and chemical characteristics to adsorption performance under different rainwater conditions. By establishing explicit links between the physicochemical properties of adsorbent materials, solution chemistry, and contaminant removal, through the critical analysis of studies conducted under comparable pH conditions and contaminant profiles, this work enables meaningful comparisons across different material classes and provides a mechanistic basis for explaining inconsistencies in the reported adsorption behavior. Therefore, this review provides a critical basis for interpreting adsorption performance in rainwater systems and

supports the selection of appropriate adsorbent materials according to different rainwater treatment objectives and intended water uses.

This review is aligned with various Sustainable Development Goals (SDGs), particularly SDG 6 (Clean Water and Sanitation), by advancing the scientific understanding of adsorbent materials for harvested rainwater treatment and supporting the safe use of this alternative water resource [18]. The assessment of adsorbent materials and their environmental sustainability is also aligned with SDG 12 (Responsible Consumption and Production) [18]. Furthermore, by emphasizing rainwater harvesting as a climate adaptation strategy that enhances urban water resilience, this review is aligned with SDG 11 (Sustainable Cities and Communities) and SDG 13 (Climate Action) [18].

2. Adsorbent Materials Applied in Rainwater Treatment

The adsorbent materials that have been investigated for rainwater treatment can be classified into three main groups according to their structural and chemical characteristics: carbon-based materials, surface-modified mineral matrices, and biosorbents. This classification provides the basis for the discussion presented in this review and is summarized in Figure 1.

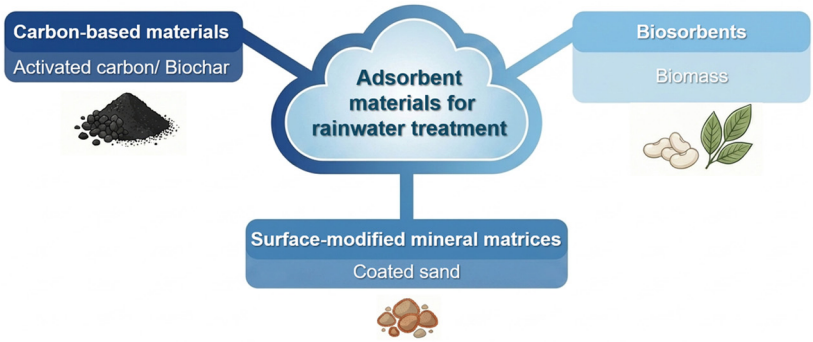


Figure 1. Schematic representation of the different classes of adsorbent materials used in the rainwater treatment process.

The studies in which adsorbent materials were applied for rainwater treatment are shown in Tables 1 and 2 and organized according to the treatment approach adopted. Table 1 includes studies in which adsorption was evaluated as an independent process, allowing assessment of the performance of the adsorbent, namely carbon-based materials, surface-modified mineral matrices, and biosorbents. Table 2 includes studies in which adsorption was combined with other treatment processes, such as filtration, oxidation, or disinfection, and the adsorbent used was carbon-based materials. In the case of Table 2, the reported removal efficiencies reflect the performance of the complete treatment system. For each study, the tables report the adsorbent class/type and its main properties, adsorption conditions, such as solution pH, contact time or flow conditions, adsorbent dose, contaminant concentration when available, target analytes or indicator parameters, and the corresponding removal efficiencies. Whenever available, pH values measured before and after adsorption are reported separately to provide an interpretation of the treatment performance. As shown in Tables 1 and 2, the studies differ in experimental conditions, such as the adsorbent materials investigated, target analytes, contaminant concentrations, pH, adsorbent dose, and contact conditions. Such differences make direct comparison of the reported removal efficiencies difficult. Information on the intended application of the treated rainwater and the sampling location is also provided in Tables 1 and 2.

Table 1. Removal efficiencies of inorganic species and organic matter from harvested rainwater using adsorbent materials.

Adsorbent		Adsorption Condition					Target Analytes/ Indicator Parameters	Removal Efficiencies (%)	Post-Treatment Use of Rainwater	Sampling Location	References
Class/Type	Properties	pH Before	pH After	Contact Time/Flow	Dose	Concentration of Analytes					
Carbon-based materials											
Biochar	Surface area: 1614 m^2/g Pore diameter: 0.8 nm pH_{PZC} = 9.3 Source: silk cocoon	7.2	N.R.	0.5–20 min (30–1200 seg) 10–180 min	3 g/L 3 g/L	1 mg/L 4 mg/L 4 mg/L 4 mg/L	Benzotriazole Zn^{2+} Cu^{2+} Ni^{2+}	93 47 99 80	N.R.	Tychy, Poland	[19]
GAC	Particle size: 12–40 mesh	7.0	7.0	1.5 L/h (25 mL/min.)	N.R.	3.13 mg/L 0.0064 cm^{-1}	OM (DOC) OM (UV_{254})	51 30	N.R.	Shanghai, China	[20]
GAC	Pore diameter: <17,300 nm (17.3 µm) Particle size: 1 to 2.36 mm Source: coconut shell	6.3–7.0	6.5–7.1	25.0 L/h (417 mL/h)	N.R.	1.54–2.77 mg/L 8.25–8.78 mg/L 0.05–0.81 mg/L	OM (BOD_5) O_2 (DO) N (NH_3-N)	43–57 3–11 72–93	Drinking water	Selangor, Malaysia	[21]
GAC	Nominal size: 0.3 mm Surface area: 1.11 m^2/g Bulk density: 748 kg/m^3 Pore diameter: 2.61 nm (26.1 Å)	5.4–8.6	N.R.	4.5 $L/m^2/h$ (lab.)	1496.0 g * (lab.)	16.0 µg/L(lab.) 9.40 mg/L (lab.)	Pb^{2+} OM (DOC)	25 (lab.) 55 (lab.)	Domestic purposes	Sydney, Australia	[22]
GAC	Nominal size: 0.3 mm Surface area: 1.11 m^2/g Bulk density: 748 kg/m^3 Pore diameter: 2.61 nm (26.1 Å)	5.4–8.6	N.R.	0.47 $L/m^2/h$ (pilot)	299.2 g * (pilot)	11.0 µg/L (pilot) 0.42 mg/L (pilot)	Pb^{2+} OM (DOC)	55 (pilot) 71 (pilot)	Domestic purposes	Sydney, Australia	[22]
GAC	Nominal size: 0.3 mm Surface area: 1.11 m^2/g Bulk density: 748 kg/m^3 Pore diameter: 2.61 nm (26.1 Å)	5.7–6.5	N.R.	0.47 $L/m^2/h$	299.2 g *	11.0 µg/L 4.0 µg/L 6.0 µg/L 2.0 µg/L 11.0 µg/L 33.0 µg/L 0.42 mg/L	Al^{3+} Cu^{2+} Fe^{2+}/Fe^{3+} Mn^{2+} Pb^{2+} Zn^{2+} OM (DOC)	9 * N.A. N.A. N.A. 55 * N.A. 71 *	Domestic purposes	Sydney, Australia	[23]
GAC	N.R.	6.3 (5.5–7.1)	N.R.	30 L/h	N.R.	4.79 mg/L 5.95 mg/L 5.40 mg/L 0.086 cm^{-1}	OM (COD) OM (TOC) OM (DOC) OM (UV_{254})	23 28 29 30	Drinking water	Salerno, Italy	[24]

Table 1. *Cont.*

Adsorbent		Adsorption Condition					Target Analytes/ Indicator Parameters	Removal Efficiencies (%)	Post-Treatment Use of Rainwater	Sampling Location	References
Class/Type	Properties	pH Before	pH After	Contact Time/Flow	Dose	Concentration of Analytes					
Surface-modified mineral matrices											
Iron hydroxide-coated sand	Specific gravity: 2.59 Bulk density: 1590 kg/m^3 Specific surface area: 15.40 m^2/g Particle size: 300–800 µm pH_{pzc}: 8.6	6.6	6.9 (6.7–7.2)	30 min. 2.45 mL/min.	117.0 g *	2200.0 µg/L 140.0 µg/L	Zn^{2+} Pb^{2+}	91 * 93 *	Domestic purposes	N.R.	[15]
Manganese oxide-coated sand + Iron hydroxide-coated sand	Specific gravity: 2.49 Bulk density: 1500 kg/m^3 Specific surface area: 1.51 m^2/g Particle size: 300–800 µm pH_{pzc}: 6.4	6.6	6.9 (6.8–7.1)	30 min. 2.45 L/min.	110.4 g *	2200.0 µg/L 140.0 µg/L	Zn^{2+} Pb^{2+}	97 * 93 *	Domestic purposes	N.R.	[15]
Iron hydroxide-coated sand	Particle size: 300–800 µm	6.5–6.9	N.R.	15 min. 4.91 mL/min.	N.R.	3600.0 µg/L 110.0 µg/L	Zn^{2+} Pb^{2+}	>97 * >91 *	Domestic purposes	N.R.	[25]
Biosorbent											
White beans *Phaseolus vulgaris* L. (peel)	Functional groups: O–H, N–H, C=O, C–N, C–O, C=C, C–O–H, P=O Elemental composition: Si, Ca	5.8–6.3 5.8–6.3	N.R. N.R.	6 h 6 h	1 bean peel 1 bean peel	100.0 µg/L 100.0 µg/L 100.0 µg/L 500.0 µg/L 500.0 µg/L 500.0 µg/L	Zn^{2+} Cu^{2+} Pb^{2+} Zn^{2+} Cu^{2+} Pb^{2+}	38–83 11–48 11–89 32–89 23–78 35–97	Domestic purposes (objective)	Estarreja, Portugal	[26]
White beans *Phaseolus vulgaris* L. (entire)	Functional groups: O–H, N–H, P=O, C=O (core), COO^-, P=S (core), C–O–C (peel) Elemental composition: Si, Ca; K, P	5.1–6.4	N.R.	2 h	5 entire beans	100.0 µg/L 500.0 µg/L	Zn^{2+} Zn^{2+}	58–85 65–69	Domestic purposes (objective)	Estarreja, Portugal	[16]
Leaves of *Tecomella undulata*	Particle size of 66.7 µm pH_{pzc}: 4.0 Functional groups: –OH, $–NH_2$, –NH, –C–N, –C=O, –CO, –CH	7.0	N.R.	43 min.	3.65 g/L	215–414 µg/L 125–241 µg/L	As^{III} As^{V}	71–99 87–98	Agricultural and drinking purposes	Nagarparkar, Pakistan	[27]

Notes: * Values calculated from the data provided in the original paper; GAC—Granular activated carbon; DOC—Dissolved organic carbon; COD—Chemical oxygen demand; TOC—Total organic carbon; BOD—Biochemical oxygen demand; DO—Dissolved oxygen; UV—Ultraviolet; lab.—Laboratory; N.A.—not applied; N.R.—not reported.

Table 2. Removal efficiencies of inorganic species and organic matter from harvested rainwater in integrated treatment systems combining adsorption with other processes.

Adsorbent		Adsorption Condition					Target Analytes/ Indicator Parameters	Removal Efficiencies (%)	Post-Treatment Use of Rainwater	Sampling Location	References
Class/Type	Properties	pH Before	pH After	Contact Time/Flow	Dose	Concentration of Analytes					
Carbon-based Materials											
AC + two polypropylene filters + UV lamp	N.R.	6.3–7.8	6.5–7.5	N.R.	N.R.	0.096 mg/L (0.040–0.150) mg/L 0.011 mg/L (0.007–0.023) mg/L	NH_4^+ NO_2^-	39 28	Non-potable uses	Zwierzyniec, Poland	[17]
AC + two polypropylene filters + UV lamp	N.R.	6.3–7.8	6.5–7.5	N.R.	N.R.	1.780 mg/L (0.240–3.230) mg/L 365.0 µg/L (112.0–700.0) µg/L	NO_3^- Cu^{2+}	20 7			
GAC + sand (SF)	Particle size: 12–40 mesh	7.0	7.0	1.5 L/h (25 mL/min.)	N.R.	3.130 mg/L 0.0064 cm^{-1} 0.340 mg/L	OM (DOC) OM (UV_{254}) N (DON)	64 (SF + GAC) 77 (SF + GAC) 84 (GAC + SF) 98 (SF + GAC)	N.R.	Shanghai, China	[20]
GAC + mollusk sand + gravel	Particle size: 0.2 to 5 mm Source: coconut shell	5.2 (4.6–6.1)	7.0 (6.3–7.4)	N.R.	N.R.	131.7 µg/L (3.2–363.0) µg/L	Pb^{2+}	100	Drinking water	West Kalimantan, Indonesia	[28]
GAC + Zeolite + UV disinfection system	Particle size: 1.2 to 1.6 mm	6.2	7.6	2.5 m/h	N.R.	<1.0 µg/L <0.1 µg/L 280.0 µg/L 30.0 µg/L <0.05 µg/L <1.0 µg/L 2.0 mg/L 2.0 mg/L <5.0 mg/L	As^{III}/As^{V} Cd^{2+} Zn^{2+} Al^{3+} Hg^{2+} Pb^{2+} OM (TOC) OM (DOC) OM (BOD_5)	N.A. N.A. 99 * 67 * N.A. N.A. >50 * >50 * N.A.	Drinking water	New South Wales, Australia	[29]
GAC + sand + gravel + rolled pebble	Specific mass: 1.27 g/cm^3 Bulk density: 630 kg/m^3	6.5 (5.5–7.3)	6.8 (6.1–7.3)	N.R.	N.R.	0.53 mg/L (0.02–1.93) mg/L 0.04 mg/L (0.01–0.11) mg/L 4.37 mg/L (1.40–15.90) mg/L 0.48 mg/L (0.07–1.80) mg/L	NH_3 NO_2^- NO_3^- PO_4^{2-}	34 N.A. 10 38 *	Non-potable uses	Santa Catarina, Brazil	[30]
GAC + membrane	Particle size: 0.38 to 0.83 mm Surface area: 941 m^2/g	7.0–7.5	N.R.	3.2 L/m^2h	N.R.	3.50 mg/L (0.11–0.12) cm^{-1}	OM (DOC) OM (UV_{254})	37 64–67 *	N.R.	Harbin, China	[31]
GAC + gravel + sand	Pore diameter: <17,300 nm (17.3 µm) Particle size: 1 to 2.36 mm Source: coconut shell	6.3–7.0	6.6–7.2	87 min 25.0 L/h (417 mL/h)	N.R.	(1.54–2.77) mg/L (8.25–8.78) mg/L (0.05–0.81) mg/L	OM (BOD_5) O_2 (DO) N (NH_3-N)	47–62 5–12 94–100	Drinking water	Selangor, Malaysia	[21]
GAC + membrane	Nominal size: 0.3 mm Surface area: 1.11 m^2/g Bulk density: 748 kg/m^3 Pore diameter: 2.61 nm (26.1 Å)	5.4–8.6	N.R.	4.5 L/m^2/h (lab.)	1496.0 g * (lab.)	16.0 µg/L (1.0–31.0) µg/L (lab.) 9.40 mg/L (2.17–13.26) mg/L (lab.)	Pb^{2+} OM (DOC)	>93 (lab.) 80 (lab.)	Domestic purposes	Sydney, Australia	[22]

Table 2. *Cont.*

Adsorbent		Adsorption Condition					Target Analytes/ Indicator Parameters	Removal Efficiencies (%)	Post-Treatment Use of Rainwater	Sampling Location	References
Class/Type	Properties	pH Before	pH After	Contact Time/Flow	Dose	Concentration of Analytes					
GAC + membrane	Nominal size: 0.3 mm Surface area: 1.11 m^2/g Bulk density: 748 kg/m^3 Pore diameter: 2.61 nm (26.1 Å)	5.4–8.6	N.R.	0.47 $L/m^2/h$ (pilot)	299.2 g * (pilot)	11.0 µg/L (pilot) 0.42 mg/L (0.16–0.84) mg/L (pilot)	Pb^{2+} OM (DOC)	55 (pilot) 78 (pilot)	Domestic purposes	Sydney, Australia	[22]
GAC + membrane	Nominal size: 0.3 mm Surface area: 1.11 m^2/g Bulk density: 748 kg/m^3 Pore diameter: 2.61 nm (26.1 Å)	5.7–6.5	N.R.	0.47 $L/m^2/h$	299.2 g *	11.0 µg/L 4.0 µg/L 6.0 µg/L 2.0 µg/L 11.0 µg/L 33.0 µg/L 0.42 mg/L	Al^{3+} Cu^{2+} Fe^{2+}/Fe^{3+} Mn^{2+} Pb^{2+} Zn^{2+} OM (DOC)	>55 N.A. >16 >50 55 N.A. 78	Domestic purposes	Sydney, Australia	[23]
GAC + membrane + UV light	N.R.	6.3 (5.5–7.1)	N.R.	30 L/h	N.R.	4.79 mg/L 5.95 mg/L 5.40 mg/L 0.086 cm^{-1}	OM (COD) OM (TOC) OM (DOC) OM (UV_{254})	50 43 37 38	Drinking water	Salerno, Italy	[24]
PAC + $KMnO_4$	Particle size: 300–400 mesh	(7.0–8.0)	N.R.	N.R.	10 mg/L	(2.85–5.68) mg/L	OM (COD_{Mn})	57	N.R.	Northwest Loess tableland, China	[32]
GAC + Silver ionizing	N.R.	6.6 (6.0–7.3)	6.8 (6.3–7.1)	N.R.	N.R.	11.00 mg/L (3.00–25.00) mg/L 3.80 mg/L (2.800–4.70) mg/L 7.58 mg /L (0.85–16.45) mg /L 1.52 mg /L (0.72–3.32) mg /L 0.36 mg /L (0.11–0.82) mg /L 3.23 mg /L (0.19–9.44) mg /L 0.04 mg /L (0.02–0.06) mg /L 0.23 mg /L (0.07–0.54) mg /L 1.48 mg /L (0.63–2.52) mg /L 3.84 mg /L (1.42–8.59) mg /L 4.51 mg /L (2.04–9.77) mg /L	OM (COD) O_2 (DO) Ca^{2+} K^+ Mg^{2+} Na^+ P F^- Cl^- NO_3^- SO_4^{2-}	41 26 * N.A. 7 * N.A. N.A. 70 * N.A. N.A. 4 * N.A.	Drinking water	San Miguel de Allende, Mexico	[33]

Notes: * Values calculated from the data provided in the original paper; AC—Activated carbon; GAC—Granular activated carbon; PAC—Powder activated carbon; DOC—Dissolved organic carbon; COD—Chemical oxygen demand; TOC—Total organic carbon; BOD—Biochemical oxygen demand; DO—Dissolved oxygen; UV—Ultraviolet; lab.—Laboratory; N.A.—not applied; N.R.—not reported.

The geographical distribution of the sampling rainwater sites included in Tables 1 and 2 is highlighted in Figure 2. Although research on adsorption for rainwater treatment has increased in recent years, the available studies are limited to a small number of regions, underlining the need for further investigations under different geographical and environmental conditions.

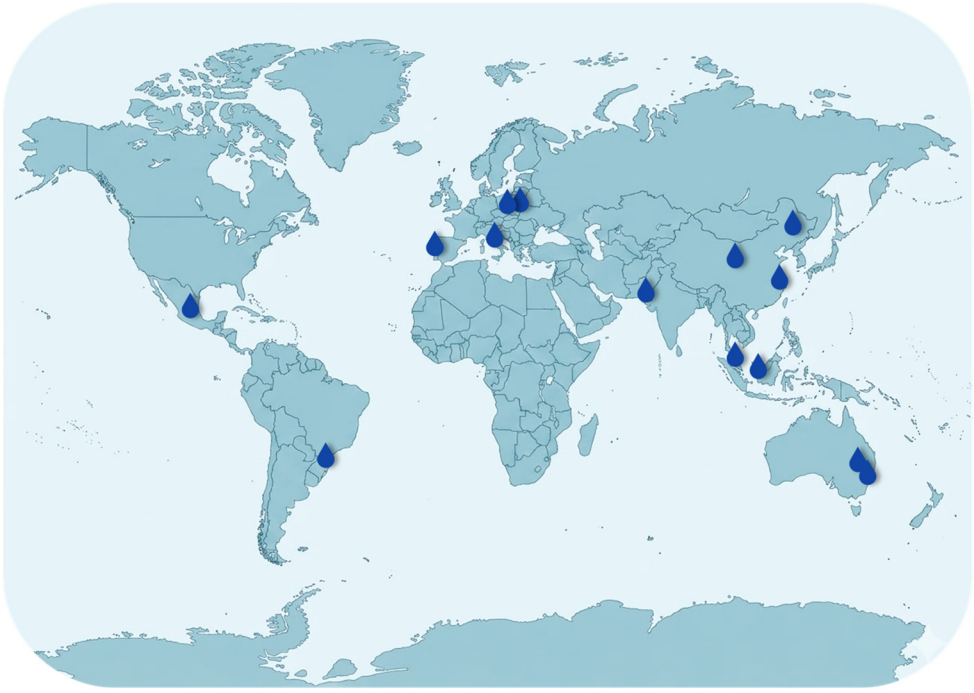


Figure 2. Geographical distribution of rainwater collection sites used in adsorption treatment studies, with blue droplets indicating the reported sampling locations.

Regarding the post-treatment use of rainwater, around 33% of the reviewed studies aimed to produce water suitable for drinking purposes, 33% of the studies focused on domestic applications, 11% investigated for non-potable purposes, while 22% did not report the post-treatment use (see Supplementary Materials Figure S1). These findings suggest that adsorption-based rainwater treatment is increasingly being developed to support higher-value water uses rather than solely improving individual water quality parameters. Moreover, this trend is reinforced by studies that have evaluated adsorption-based treatment systems under real operating conditions. Adler et al. [33] reported integrated rainwater harvesting systems operating in schools and rural health centers located in the semi-arid region of Mexico for more than one year, whereas Senevirathna et al. [29] monitored a fully automated solar-powered treatment plant supplying drinking water to approximately 125 users over 30 months of continuous operation. In addition, Khayan et al. [28], Teixeira and Ghisi [30], Grabowski et al. [17], Naddeo et al. [24], and Kus et al. [22,23] evaluated pilot- or full-scale treatment systems operating for periods ranging from approximately four months to one year. These studies demonstrate the practical applicability of adsorption-based rainwater treatment under realistic operating conditions and support its potential for implementation in rainwater harvesting systems.

In what concerns the classes of adsorbent materials studied for rainwater treatment, the most published studies have focused on carbon-based materials (72%), whereas surface-modified mineral matrices (11%) and biosorbents (17%) have received substantially less attention (see Supplementary Materials Figure S1). Concerning the type of contaminants, carbon-based materials have been investigated for the removal of organic matter (69% of the studies), potentially toxic elements (46%), major ions (23%), and organic micropollutants

(8%). On the other hand, surface-modified mineral matrices and biosorbents have been evaluated exclusively for potentially toxic element removal.

2.1. Carbon-Based Materials

Carbon-based materials are widely employed in water treatment due to their high surface area and versatile surface chemistry, which enables the removal of a broad range of contaminants [34]. Several types of carbon-based materials have been developed, including activated carbon (AC), biochar, carbon nanotubes, and graphene-based materials [35]. The studies compiled in Tables 1 and 2 highlight that AC is the predominant carbon-based material investigated for rainwater treatment. In Table 1, AC is evaluated alongside a single study on biochar, whereas Table 2 includes only studies combining AC with other treatment processes.

2.1.1. Activated Carbon/Biochar

AC and biochar are porous carbonaceous adsorbent materials widely investigated for water treatment due to their [34] well-developed pore structure, large specific surface area, and versatile surface chemistry, which together provide a high density of adsorption sites for the removal of a wide range of organic and inorganic contaminants [36,37] AC is an engineered porous carbon material widely used in adsorption applications due to its well-developed pore network and surface chemistry, which provide a high density of accessible adsorption sites for contaminant removal [37]. Biochar is a carbon-rich material obtained from the thermochemical conversion of biomass that generally preserves structural features and inorganic constituents derived from the original biomass, thereby influencing its physicochemical properties and adsorption behavior [36,38]. Although both materials can originate from similar carbon-rich precursors, differences in their production pathways and physicochemical characteristics result in distinct adsorption behavior, contaminant interactions, and removal performance under different treatment conditions [37,38].

Preparation and Physicochemical Characteristics of Activated Carbon/Biochar

The preparation route is one of the main factors determining the physicochemical characteristics and adsorption performance of carbonaceous adsorbents. Although activated carbon (AC) and biochar originate from carbon-rich precursors converted through thermochemical processes, differences in their production pathways result in distinct degrees of pore development, surface functionality, and adsorption behavior. The production of AC generally involves three sequential stages: precursor preparation, carbonization, and activation [39]. Precursor preparation includes cleaning, drying, and particle size reduction to ensure material uniformity. Carbonization converts the precursor into a carbon matrix under inert or oxygen-limited conditions, removing volatile components and forming an initial porous structure. The activation step is critical for defining the final physicochemical properties of AC, as it develops porosity, enlarges existing pores, and introduces surface functional groups. Activation can be performed through physical methods, typically using steam or gases such as carbon dioxide at high temperatures [40–42], chemical methods involving agents such as NaOH, K_2CO_3, or $CaCl_2$ followed by thermal treatment [43–45] or by combining both methods. These different activation strategies lead to variations in pore size distribution, specific surface area, and surface chemistry, which directly influence adsorption mechanisms and contaminant removal efficiency.

Biochar is generally produced through pyrolysis of biomass under oxygen-limited conditions, with its properties strongly influenced by precursor composition and operating parameters, including temperature, heating rate, and residence time. Compared with conventional AC production, biochar preparation usually does not involve an additional activation step aimed at maximizing porosity. Therefore, biochar often retains a higher

proportion of oxygen-containing functional groups and inorganic constituents derived from the original biomass, which may contribute to adsorption through mechanisms such as surface complexation, electrostatic interactions, and ion exchange [36,38]. However, activation treatments can substantially modify biochar characteristics by increasing surface area and pore development, producing materials with properties closer to activated carbon.

The influence of preparation conditions on material properties is evident in the adsorption performance of carbonaceous adsorbents. Parameters such as precursor type, carbonization temperature, activation method, and chemical treatment determine pore structure, surface functionality, and adsorption site availability. Therefore, classification based solely on the material designation (AC or biochar) may not fully explain adsorption behavior, since the final physicochemical properties are strongly dependent on the preparation conditions.

Despite these well-established production pathways, most studies compiled in Tables 1 and 2 depend on commercial AC or do not report its origin. Only Shaheed et al. [21] and Khayan et al. [28] provide explicit information on AC preparation, both using coconut shell as precursor material. Shaheed et al. [21] produced AC via pyrolysis at 700 °C for 1.5 h followed by chemical activation using sodium chloride. In contrast, Khayan et al. [28] applied a multi-step thermal process involving dehydration at 170 °C, partial decomposition at 275 °C, and carbonization above 400 °C, achieving approximately 80% carbon yield prior to chemical activation with calcium chloride. These differences highlight how variations in thermal and chemical activation routes can lead to distinct carbon structures, which are expected to influence adsorption behavior through differences in porosity development and surface chemistry.

The only study investigating biochar in rainwater treatment was reported by Marszałek et al. [19]. The authors prepared the biochar from waste silkworm cocoons through carbonization followed by chemical activation with KOH and high-temperature thermal treatment under a nitrogen atmosphere. Although the material was described as biochar by the authors, its preparation involved both carbonization and activation steps, which are known to strongly influence pore development and surface chemistry.

The physicochemical properties of AC are fundamental to its performance in water treatment, as they govern adsorption capacity, mass transfer, and hydraulic behavior. Relevant parameters such as particle size, specific surface area, pore volume, pore size distribution, and bulk density control pore accessibility and strongly influence both adsorption kinetics and operational performance. These characteristics also determine the form in which AC is applied in treatment systems. Accordingly, AC is commonly classified according to morphology and particle size into powdered activated carbon (PAC), granular activated carbon (GAC), activated carbon fibers (ACF), and activated carbon cloth (ACC) [46].

As shown in Tables 1 and 2, reporting of AC physical properties is highly variable and often incomplete. GAC is the most frequently applied form across the reviewed studies, and particle size is the most consistently reported parameter. However, values vary widely, from 0.3 mm [22,23], in which particle size is reported as a nominal value that likely reflects a commercial specification rather than an experimentally determined particle size distribution, to 0.38–0.83 mm [31], 1–2.36 mm [21], 12–40 mesh [20], corresponding approximately to sieve openings between 1.70 and 0.425 mm, 1.2–1.6 mm [29], and 0.2–5 mm [28]. This variability in particle size is relevant because it directly affects hydraulic conductivity and adsorption kinetics: smaller particles enhance mass transfer and external surface accessibility, whereas larger particles improve flow conditions but may limit adsorption rate due to longer diffusion pathways.

Other physical parameters are less consistently reported. Specific surface area is available only for a subset of studies and ranges from 1.11 m^2/g for AC reported by Kus et al. [22,23] to 941–1050 m^2/g for AC reported by Ding et al. [31]. The only biochar evaluated in this review exhibited a specific surface area of 1614 m^2/g [19]. These differences are consistent with the use of different precursor materials, activation procedures, and characterization methods across studies. Since surface area determines the number of available adsorption sites, materials with higher values generally exhibit greater adsorption capacity and improved mass transfer. Regarding the bulk density, it was presented in the studies of Kus et al. [22,23] and Teixeira & Ghisi [30], having varied between 630 and 748 kg/m^3, which suggests differences in packing behavior. Lower bulk density suggests more porous bed structures with higher void fraction, potentially enhancing flow distribution and contact time, whereas higher values imply more compact packing and increased resistance to flow. Pore structure data show even greater variability, with reported pore diameters ranging from values below 2.61 nm [22,23] to approximately 17,300 nm [21]. According to the International Union of Pure and Applied Chemistry (IUPAC), pore diameters are classified as micropores (<2 nm), mesopores (2–50 nm), and macropores (>50 nm) [47,48]. Based on this classification, the reported pore diameters for AC are within the mesopore (2.61 nm) and macropore (17,300 nm) size ranges. The biochar evaluated by Marszałek et al. [19] exhibited an average pore diameter of 0.8 nm, corresponding to the micropore range. These differences in pore structure are expected to influence adsorption behavior, since pore size governs the accessibility of adsorption sites and the diffusion of contaminants within the adsorbent [37].

Beyond physical characteristics, adsorption performance is also strongly influenced by the chemical nature of AC. Surface functional groups such as hydroxyl (-OH), carboxyl (-COOH), carbonyl/quinone (C=O), phenolic, and lactone groups provide active sites for interactions with contaminants [49]. The surface charge, governed by the point of zero charge (pH_{PZC}), typically ranges from 4.8 to 8.2 depending on precursor and activation conditions [50], controls electrostatic interactions with ionic species under different pH conditions. These combined chemical and structural features enable AC to remove both organic and inorganic contaminants via adsorption and physical retention.

A critical limitation identified across the reviewed studies is the absence of systematic and comparable characterization of AC, particularly regarding surface functional groups, pH_{PZC}, particle size distribution, surface area, and pore structure. Although AC is generally assumed to exhibit broadly similar intrinsic chemical features, the inconsistent reporting of these parameters prevents a coherent interpretation of how material properties govern adsorption behavior under rainwater conditions. This limitation becomes critical when attempting to relate material properties to observed removal efficiencies, since key descriptors governing adsorption mechanisms are often missing or partially reported. As a result, variations in performance cannot be reliably linked to specific physicochemical characteristics, even though particle size and pore structure control mass transfer and site accessibility, surface area and functional groups determine the density and reactivity of adsorption sites, and pH_{PZC} governs electrostatic interactions under variable pH conditions. Consequently, reported differences in removal performance reflect not only material-dependent behavior but also inconsistencies in experimental design and reporting practices. This compromises the development of reliable structure–performance relationships and limits the transferability of findings across studies. A more standardized reporting framework for activated carbon characterization is therefore essential to improve comparability and support mechanistic interpretation in rainwater treatment research.

Applications of Activated Carbon/Biochar in Rainwater Treatment

Tables 1 and 2 evidence that AC has been widely applied in harvested rainwater treatment. The studies compiled in Table 1 provide an overview of the performance of AC applied as a standalone treatment unit for harvested rainwater, while Table 2 presents configurations in which AC was combined with additional media or processes, including sand, gravel, zeolites, rolled pebbles, membrane filtration, potassium permanganate ($KMnO_4$), silver ionization, or ultraviolet (UV) disinfection. This distinction is critical, since removal efficiencies reported for integrated systems cannot be unequivocally attributed to adsorption by AC alone. Moreover, GAC is the most often employed form, whereas PAC and biochar are less commonly reported.

The studies summarized in Table 1 show that GAC can reduce both organic and inorganic constituents. This variability reflects not only differences in water composition and operational conditions, but also the influence of pH on both the surface chemistry of GAC and the speciation of dissolved compounds. The pH of harvested rainwater reported in these studies ranged from approximately 5.2 to 8.6. Within this interval, the apparent performance of GAC may reflect not only adsorption but also additional removal processes, depending on the nature of the contaminants and the system operating conditions. For example, physical filtration may contribute to the removal of suspended particulate material [51], precipitation may influence the removal of specific inorganic species [52], and, in long-term operating systems, biologically mediated degradation may contribute to the removal of organic matter following the development of microbial biofilms [31]. Consequently, the reported removal efficiencies do not necessarily reflect the intrinsic adsorption capacity of GAC alone but may instead represent the combined contribution of concurrent removal mechanisms.

Under these conditions, the evaluation of GAC performance in harvested rainwater treatment has been studied for the removal of organic matter (OM), in addition to the removal of potentially toxic elements, given the ubiquitous presence and its relevance as a precursor for potentially harmful by-products during storage or subsequent treatment. Regarding the removal of OM, the studies rely mainly on bulk parameters, including dissolved organic carbon (DOC), total organic carbon (TOC), chemical oxygen demand (COD), UV_{254} absorbance, and biochemical oxygen demand (BOD_5). Although these indicators provide complementary information on OM concentration, aromaticity, and biodegradability, they are bulk water quality parameters and therefore do not provide direct evidence of the mechanisms responsible for OM removal. Consequently, the relative contributions of adsorption and other concurrent removal processes cannot be distinguished from these parameters alone, particularly in the absence of experimental approaches designed to isolate individual mechanisms.

For OM, the removal efficiencies reported for standalone GAC systems show pronounced variability, even under similar pH conditions. Dissolved organic carbon (DOC) removal ranges from approximately 29% to 71% across a pH interval of 5.4 to 8.6 [20,22–24]. He et al. [20] reported a 51% reduction in DOC at pH 7.0, whereas Kus et al. [22,23] obtained higher removals of 55% to 71% over a broader pH range of 5.4 to 8.6. Moreover, comparison of the laboratory and pilot-scale systems reported by Kus et al. [22,23]. Laboratory-scale experiments with a higher activated carbon dose (1496 g, calculated from Kus et al. [22]) achieved 55% DOC removal. In contrast, pilot-scale operation at a substantially lower dose (299 g, calculated from Kus et al. [22]) resulted in 71% DOC removal. This behavior cannot be explained solely by adsorbent dosage. This behavior may be explained by adsorbent dosage together with flow, which was 4.5 L m^{-2} h^{-1} and 0.47 L m^{-2} h^{-1} for the laboratory and pilot-scale systems, respectively. On the other hand, Naddeo et al. [24] reported consistently lower OM removal, with reductions of 23% for COD, 28% for TOC, 29% for DOC,

and 30% for UV_{254}, across a pH range of 5.5 to 7.1. Although these pH values fall within the same general interval reported in other studies, the markedly lower removal efficiencies suggest that pH alone does not account for the observed differences. These findings may be due to the high flow rate when compared with the remaining studies, which was 30 L h^{-1}. Moreover, differences in DOM composition and characteristics may have also influenced GAC performance. Furthermore, differences in treatment configuration may also contribute to the observed variability in OM removal. Wu et al. [32] achieved 57% COD_{Mn} removal when PAC adsorption was preceded by $KMnO_4$ pre-oxidation at pH 7.0–8.0. The authors attributed this performance to changes in the characteristics of OM, which enhanced its adsorption. Therefore, the reported removal efficiencies also depend on the treatment configuration. At the same time, direct comparisons between PAC and GAC remain limited due to differences in experimental design, flow, dose and reporting methods.

Since adsorption alone does not fully explain OM removal, additional processes must be considered. In this context, variations in dissolved oxygen (DO) provide relevant insight into the occurrence of biologically mediated mechanisms. DO does not directly reflect OM removal but rather reflects the balance between oxygen availability, microbial respiration, and system aeration conditions. Shaheed et al. [21] reported decreases in DO ranging from 3.0% to 11% in systems using GAC. These changes were accompanied by BOD_5 reductions between 43% and 57% and NH_3–N removal between 72% and 93%. The experiments were conducted at a pH range between 6.3 and 7.0, conditions favorable to aerobic microbial activity. In addition, the combination of GAC with gravel and sand filtration (Table 2) resulted in DO decreases of 5% to 12%, reflecting slightly increased oxygen consumption associated with enhanced biological processes.

Further insight into the role of biodegradation is provided by studies examining biomass development and temporal trends in OM removal (Table 2). Ding et al. [31] reported substantial accumulation of biomass and extracellular polymeric substances on GAC, with more than 80% of the biomass associated with previously adsorbed organic matter, supporting the occurrence of active microbial degradation. In addition, Kus et al. [23] observed a gradual improvement in DOC removal over time under stable conditions, reflecting the progressive establishment of biologically active systems. Long-term operation of a GAC–zeolite system for 30 months without regeneration or disinfection further supports the persistence of biofilm-mediated processes [29].

Although microbial activity appears to contribute to OM removal, its magnitude remains difficult to quantify. For example, Areerachakul et al. [53] attributed up to 40% of DOC removal to biological processes in a submerged membrane–biofilter system, where the solid matrix functioned primarily as a support for biofilm development. However, the absence of experimental controls that separate adsorption from biodegradation prevents a clear distinction between the mechanisms. Additional evidence is provided by DO behavior in integrated systems (Table 2), namely Adler et al. [33] reported a decrease of 26% in DO after treatment with GAC combined with silver ionization, a value calculated from the data reported in the original study. This reduction in DO is due to oxygen consumption under conditions of limited aeration and supports the contribution of microbial respiration.

Therefore, DO variations should be interpreted as an indirect indicator of biological activity rather than as a direct measure of OM removal. Consequently, under typical operating conditions, GAC-based systems may involve simultaneous adsorption, biodegradation, and physical retention processes, which complicate the interpretation of removal efficiencies and may lead to an overestimation of the material's intrinsic adsorption capacity.

In contrast to organic matter, whose removal in GAC systems often reflects the combined contribution of adsorption and biologically mediated processes, the removal of inorganic constituents allows a more direct evaluation of physicochemical interactions,

although additional processes may still occur depending on system configuration. In harvested rainwater, inorganic species, particularly metals, are commonly associated with atmospheric deposition and the degradation of roofing materials, which explains their frequent evaluation across the studies analyzed.

The interpretation of removal efficiencies remains strongly dependent on solution chemistry, particularly pH. This parameter controls both the speciation of dissolved metals and the surface charge and functional groups of GAC, thereby influencing the dominant removal pathways. According to the studies considered, pH values generally range from 5.2 to 8.6, a range in which several metals may hydrolyze or form insoluble hydroxide species [52]. As a result, removal may occur not only by adsorption but also through the retention of colloidal or particulate species, making the dominant removal mechanism more difficult to identify. Pb^{2+} provides a good example of this effect. Kus et al. [22] reported removal efficiencies of 25% using GAC alone at laboratory scale, increasing to 55% after membrane integration. At pilot scale, removal increased from 55% with GAC to more than 93% when combined with membrane filtration. Besides membrane integration, the higher Pb^{2+} removal observed at pilot scale may also be related to the lower flow rate (0.47 L m^{-2} h^{-1}) compared with the laboratory-scale experiments (4.5 L m^{-2} h^{-1}), which increases the contact time between rainwater and GAC. Moreover, the experiments were conducted at pH values between approximately 5.4 and 8.6, where Pb^{2+} may hydrolyze to species such as $Pb(OH)^{+}$ and $Pb(OH)_2$ [52]. Therefore, part of the reported removal may result from physical retention rather than adsorption alone. These transformations reduce the fraction of free Pb^{2+} available for adsorption onto GAC and favor the presence of colloidal or particulate forms in solution. Under such conditions, part of the observed removal may be due to physical retention rather than direct adsorption.

The behavior of Cu^{2+} and Zn^{2+} was considerably less consistent than that observed for Pb^{2+}. Kus et al. [23], at pilot scale, reported increases of 3.5% for Cu^{2+} and 15% for Zn^{2+} (calculated from the available data) after treatment with GAC, while membrane integration did not improve their removal. These findings suggest that the treatment system itself may have acted as a source of these metals, which is undesirable in water treatment applications. In other studies, however, Cu^{2+} and Zn^{2+} removal was achieved using carbon-based adsorbents. Grabowski et al. [17] reported approximately 7% Cu^{2+} removal in a treatment system combining AC, polypropylene filters, and UV irradiation, whereas Senevirathna et al. [29] achieved Zn^{2+} removal close to 99% using GAC combined with zeolite and UV disinfection. Marszałek et al. [19] also reported removal efficiencies of approximately 99% for Cu^{2+}, 80% for Ni^{2+}, and 47% for Zn^{2+} using biochar. The high removal efficiencies reported by Marszałek et al. [19] should also be interpreted in light of the experimental conditions. The biochar used in this study had a pH_{PZC} of 9.3, whereas the experiments were performed at pH 7.2. Under these conditions, the biochar surface is expected to remain positively charged, meaning that electrostatic attraction alone cannot explain the efficient removal of cationic metals. At the same time, solution chemistry must also be considered because metal speciation changes with pH. According to Stumm and Morgan [52], Cu^{2+}, and to a reduced extent Pb^{2+} and Zn^{2+}, begin to hydrolyze within this pH range, leading to the formation of hydroxyl species and, depending on the solution composition, the onset of hydroxide precipitation. Consequently, the high Cu^{2+} removal reported in this study may reflect not only adsorption onto the biochar surface but also the retention of hydrolyzed or particulate species. By comparison, Ni^{2+} remains predominantly as dissolved ionic species at pH 7.2, suggesting that its removal is less influenced by changes in speciation and more closely related to interactions with the biochar surface.

A similar interpretation can be extended to other metals such as Al^{3+}, Fe^{2+}/Fe^{3+}, and Mn^{2+}. Kus et al. [23] reported only 9% Al^{3+} removal with GAC alone (calculated from avail-

able data), whereas removal exceeded 55% in the GAC–membrane system. In comparison, Senevirathna et al. [29] achieved 67% Al^{3+} removal in an integrated system combining GAC, zeolite, and UV disinfection (calculated from available data). For Fe^{2+}/Fe^{3+}, Kus et al. [23] reported a 67% increase in concentration following GAC treatment (value calculated from the data reported in the study), while membrane integration resulted in removal efficiencies exceeding 16%. The same study reported no Mn^{2+} removal with GAC alone, whereas the GAC–membrane system achieved removal above 50%.

The previous observations highlight the limitations of directly comparing the reported removal efficiencies. Besides the intrinsic properties of the adsorbent, the performance of carbon-based materials is influenced by solution chemistry, hydraulic conditions, and treatment configuration. This is particularly relevant for integrated treatment systems, where the contribution of activated carbon cannot be separated from that of the accompanying treatment processes. Moreover, because pH simultaneously influences the adsorbent surface and metal speciation, similar removal efficiencies do not necessarily reflect the same removal mechanism.

The removal of inorganic anions remains a limitation in integrated treatment systems containing adsorbent materials (Table 2). The evaluated systems combined adsorption with different treatment processes, including filtration media [30], polypropylene filtration followed by UV disinfection [17], and silver ionization [33]. Teixeira & Ghisi [30] and Grabowski et al. [17] evaluated the removal of both nitrate (NO_3^-) and nitrite (NO_2^-), whereas Adler et al. [33] investigated only nitrate (NO_3^-). Despite the different treatment configurations, nitrate removal remained consistently low, ranging from 4% in Adler et al. [33] to 20% in Grabowski et al. [17], while Teixeira & Ghisi [30] reported approximately 10%. For nitrite, Grabowski et al. [17] achieved 28% removal, whereas no removal was observed by Teixeira & Ghisi [30].

For other anions, including Cl^-, SO_4^{2-}, and F^-, an increase in concentration after treatment was reported only in Adler et al. [33], reported increases in concentration after treatment of approximately 1%, 37%, and 17% (calculated from available data), respectively. These increases suggest leaching or ion exchange processes within the filter media rather than effective removal. Phosphate (PO_4^{3-}) was evaluated only in Teixeira & Ghisi [30], where a removal of 38% (calculated from available data) was observed. However, phosphate behavior is strongly dependent on system configuration and water chemistry, which may influence removal through processes such as adsorption, precipitation, or interactions with mineral components [54]. Cationic species such as NH_4^+, Ca^{2+}, Mg^{2+}, Na^+, and K^+ further illustrate the complexity of inorganic removal (Table 2). Grabowski et al. [17] reported NH_4^+ removal below 40%, whereas Adler et al. [33] observed an approximately 60% increase in Na^+ concentration and a 31% decrease in Ca^{2+} concentration after treatment, based on the reported data. These differences suggest that changes in cation concentrations are influenced by multiple processes occurring within the treatment system and cannot be attributed solely to adsorption. Such variability illustrates the complexity of inorganic contaminant removal in harvested rainwater treatment and highlights the influence of both the chemical species evaluated and the treatment configuration on the reported performance. Therefore, removal efficiencies reported for treatment systems combining GAC with other processes should be interpreted with caution, as the specific contribution of activated carbon cannot always be distinguished from that of the accompanying treatment processes.

2.2. Surface-Modified Mineral Matrices

2.2.1. Coated Sand

Coated sand consists of mineral particles whose surfaces are modified through the deposition of reactive phases, typically metal oxides or hydroxides, in order to enhance

their adsorption capacity [55]. This modification alters surface chemistry by introducing functional groups and shifting charge characteristics, thereby promoting interactions with dissolved species, particularly potentially toxic elements [56]. In comparison, uncoated sand exhibits limited chemical reactivity and is primarily associated with physical filtration rather than adsorption-driven removal.

Despite these advantages, the application of coated sand in harvested rainwater treatment remains poorly explored. Available evidence is restricted to the studies of Ahammed & Meera [15,25], which evaluated the removal of Zn^{2+} and Pb^{2+} from harvested rainwater, as shown in Table 1. Although this limited dataset constrains a comprehensive assessment, it provides a consistent experimental framework for analyzing material preparation, physicochemical properties, and adsorption performance.

Preparation and Physicochemical Characteristics of Coated Sand

The preparation of coated sand for rainwater treatment has been reported exclusively by Ahammed & Meera [15,25]. In both studies, river sand with particle sizes between 300 and 800 μm was selected as the base material due to its mechanical stability and suitability for packed-bed filtration systems. Surface modification was achieved by depositing iron hydroxide, yielding iron hydroxide-coated sand (IOCS). The study by Ahammed & Meera [15] further expanded the material scope by introducing manganese oxide-coated sand (MOCS), applied in combination with IOCS in a dual-media configuration, while uncoated sand served as a reference material. This experimental design enabled direct comparison between modified and unmodified media, as well as between single- and dual-coating strategies under comparable operating conditions.

Surface modification induced pronounced changes in physicochemical properties. Uncoated sand exhibited a low specific surface area (0.22 $m^2\ g^{-1}$) and a pH_{pzc} of 6.8. Following coating, IOCS showed a substantial increase in surface area (15.4 $m^2\ g^{-1}$) and a shift in pH_{pzc} to 8.6, indicating a predominantly positively charged surface under near-neutral conditions. Conversely, MOCS presented a lower surface area (1.51 $m^2\ g^{-1}$) and a pH_{pzc} of 6.4, suggesting a surface that may become negatively charged within the same pH range.

These variations highlight the role of coating composition in defining surface reactivity and charge behavior. Differences in pH_{pzc} suggest that electrostatic interactions with dissolved species are expected to vary substantially between materials, potentially influencing adsorption performance and selectivity depending on the contaminant and solution chemistry.

Applications of Coated Sand in Rainwater Treatment

The studies of Ahammed & Meera [15,25] focused on the removal of potentially toxic elements, namely Zn^{2+} and $Pb^{2+,}$ from harvested rainwater by coated sand, as presented in Table 1. In the study by Ahammed & Meera [25], the initial pH ranged between 6.5 and 6.9. A similar initial pH (approximately 6.6) was reported in the study by Ahammed & Meera [15]. Although conducted under comparable initial conditions, Ahammed & Meera [15] optimized contact time to 30 min for long-term experiments to ensure better performance, replacing the 15 min used in Ahammed & Meera [25]. Accordingly, the flow rate was reduced from 4.91 mL min^{-1} [25] to 2.45 mL min^{-1} [15]. Despite these operational differences, the initial metal concentrations remained comparable between studies, with Zn^{2+} concentrations ranging from 2200 to 3600 μg L^{-1} and Pb^{2+} concentrations from 110 to 140 μg L^{-1}. In both studies, the treated rainwater was intended for domestic use.

Removal efficiencies varied substantially among the filtration media. Ahammed & Meera [25] reported IOCS removal efficiencies exceeding 97% for Zn^{2+} and 91% for Pb^{2+}.

In a subsequent study, Ahammed & Meera [15] reported Zn^{2+} and Pb^{2+} removals of 91% and 93%, respectively, with IOCS alone. The dual-media configuration, consisting of MOCS layered over IOCS, increased Zn^{2+} removal to 97%, whereas Pb^{2+} removal remained unchanged. On the other hand, uncoated sand exhibited markedly lower performance, with removal efficiencies of 27% for Zn^{2+} and 29% for Pb^{2+} (these data are not included in Table 1 because uncoated sand was considered a filtration medium rather than a sorbent material, and the table only summarizes materials applied for sorption-based removal). Therefore, these results consistently demonstrate the clear advantage of surface-modified sand over uncoated sand under comparable conditions. However, the mechanisms underlying this enhanced performance require careful consideration. At the investigated pH range (6.5–6.9), both Zn^{2+} and Pb^{2+} are expected to undergo hydrolysis, leading to the formation of hydrolyzed species and, particularly for Pb^{2+}, the onset of precipitation [52]. Consequently, the reported removal efficiencies should not be interpreted exclusively as evidence of adsorption, since solution chemistry may also contribute through hydrolysis, precipitation and subsequent retention within the filter bed. Further insight into these mechanisms can be obtained by comparing the behavior of coated and uncoated sand. Uncoated sand has a pH_{pzc} of 6.8 and, because the experiments were conducted at pH values close to this condition, its surface is expected to be only weakly charged, thereby limiting electrostatic interactions with dissolved metal species. Consequently, the metal removal achieved by uncoated sand is more plausibly attributed to physical filtration and retention within the granular matrix rather than to sorption processes, which is consistent with its low specific surface area (0.22 $m^2\ g^{-1}$). In contrast, IOCS (pH_{pzc} = 8.6) exhibits different surface characteristics. In both studies by Ahammed & Meera [15,25], the reported pH values remained below the pH_{pzc} of IOCS, suggesting that its surface is expected to remain positively charged under the experimental conditions. However, this does not favor electrostatic attraction of Zn^{2+} and Pb^{2+}, suggesting that classical adsorption mechanisms alone cannot account for the observed removal efficiencies. Therefore, the high removal efficiencies are more consistently explained by the substantial increase in specific surface area (15.4 $m^2\ g^{-1}$), which enhances contact probability and promotes retention within the porous structure. Moreover, this increased surface area provides favorable conditions for heterogeneous nucleation of hydrolyzed species, followed by their retention within the granular matrix. The combination of MOCS over IOCS further supports this interpretation. Although MOCS has a pH_{pzc} of 6.4, suggesting the possibility of slightly negative surface charge at pH 6.6, its relatively low specific surface area (1.51 $m^2\ g^{-1}$) limits its contribution through sorption interactions. Therefore, the observed increase in Zn^{2+} removal is more consistently attributed to the introduction of an additional filtration layer, which enhances particle interception and modifies flow pathways before they contact the IOCS layer. On the other hand, the absence of improvement in Pb^{2+} removal suggests that its behavior is primarily governed by solution chemistry, particularly hydrolysis and the formation of low-solubility species such as $Pb(OH)^+$ and $Pb(OH)_2$ [52]. Under these conditions, precipitation and subsequent physical retention within the granular bed are expected to dominate over surface-driven adsorption processes, making the removal less sensitive to changes in filtration configuration.

The available evidence of coated sand supports a mechanistic framework in which removal is governed predominantly by physical filtration, retention within the granular matrix, and precipitation-related processes. Surface modification enhances performance primarily through increased surface area and the facilitation of phase transformation and retention, rather than through strong sorptive interactions. Nevertheless, the absence of experimental approaches designed to isolate individual mechanisms limits mechanistic resolution, and the small number of available studies restricts broader generalization.

Therefore, further investigation under controlled conditions is required to quantify the relative contribution of filtration, precipitation, and surface-mediated processes, particularly within pH ranges where metal speciation is highly sensitive to small variations.

2.3. Biosorbents

Biosorbents are biologically derived materials that have been widely investigated as alternative adsorbents for water treatment because of their ability to remove contaminants from aqueous systems while promoting the utilization of naturally occurring materials and biological resources [57,58]. Over the past decades, the range of investigated biosorbents has expanded considerably, reflecting the increasing interest in developing sustainable materials for water purification [59]. Biosorbents encompass a broad diversity of biological materials that differ in composition and structural characteristics. Based on their biological source, they can be grouped into plant biomass, microbial biomass, animal biomass, and their derivative products [60]. Plant biomass comprises materials derived from higher plants; microbial biomass includes bacteria, fungi, algae, and yeasts, whereas animal biomass encompasses materials such as chitin- and chitosan-based sorbents [58,60]. Although biosorbents comprise a wide range of biological materials, only plant biomass has been investigated for harvested rainwater treatment [16,26,27].

2.3.1. Plant Biomass

Plant biomass-based sorbents investigated for harvested rainwater treatment include leaves, whole seeds, and seed coats, although a much wider range of plant materials, such as bark, agricultural residues and other lignocellulosic materials, has been explored for water treatment applications [58,61]. To date, only three studies have investigated the use of plant biomass for this application, namely leaves of *Tecomella undulata* [27], whole white beans of *Phaseolus vulgaris* L. [16], and white bean peels of *Phaseolus vulgaris* L. [26]. The limited number of available studies reflects the current state of research on the application of plant biomass to harvested rainwater treatment. The plant biomass adsorbents investigated for harvested rainwater treatment are summarized in Table 1.

Preparation and Physicochemical Characteristics of Plant Biomass

The preparation procedures adopted for the plant biomass materials differed according to the type of material evaluated. The earliest study by Brahman et al. [27] prepared leaves of *Tecomella undulata* by successive washing, followed by drying at 60 °C for 48 h, grinding, and sieving to obtain particles smaller than 75 μm.

The subsequent studies investigated whole beans of *Phaseolus vulgaris* L. [16] and bean peels of *Phaseolus vulgaris* L. [26]. Ferreira et al. [16] evaluated whole beans and the influence of washing and drying conditions and reported that triple rinsing followed by drying at 30 °C for 24 h reduced the release of soluble organic matter, thereby improving material stability in aqueous media. Cabral et al. [26] prepared the bean peel by soaking the beans, manually separating the peels, drying them at 30 °C for 24 h according to the procedure described by Ferreira et al. [16], and storing the material in a desiccator until use. Ferreira et al. [16] and Cabral et al. [26] further showed that both the preparation procedure and the amount of biosorbent used influenced the release of organic matter into solution.

The physicochemical characteristics of the plant biomass materials were investigated using complementary analytical techniques, including Fourier transform infrared (FTIR) spectroscopy, X-ray diffraction (XRD), scanning electron microscopy (SEM), energy-dispersive X-ray spectroscopy (EDS), and pH_{PZC} determination. FTIR analysis was employed in all three studies to identify the functional groups associated with the plant biomass materials. Despite the different plant sources investigated, the spectra showed a comparable distribution of oxygen- and nitrogen-containing functional groups. Ferreira

et al. [16] and Cabral et al. [26] identified absorption bands attributed to hydroxyl (-OH), amine (-NH_2), aliphatic (C-H), carbonyl (C=O), carboxyl (-COOH), and CN-containing groups in *Phaseolus vulgaris* materials. Similarly, Brahman et al. [27] identified hydroxyl (-OH), amine (-NH_2), carbonyl (C=O), and aliphatic (C-H) groups in *Tecomella undulata* leaves. Ferreira et al. [16] further identified COO^- and P=S bands in the bean core, indicating compositional differences between the core and peel.

Additional analytical techniques were employed to investigate the structural, morphological, and elemental characteristics of the plant biomass materials. XRD analysis was only reported by Ferreira et al. [16] for whole beans, revealing a broad diffraction band between 15° and 35° (2θ), indicative of the presence of amorphous silica. SEM analysis revealed marked differences in surface morphology between the plant biomass materials. Ferreira et al. [16] observed marked differences between the bean peel and core, with the peel exhibiting a rough and irregular surface, whereas the core presented a more compact morphology. On the other hand, SEM images of the leaves revealed a heterogeneous surface with numerous cavities and irregularities [27], providing potential sites for interaction with contaminants.

Elemental composition was investigated using EDS. Ferreira et al. [16] reported higher proportions of Si and Ca in the bean shell, whereas K and P were more abundant in the bean core. Particle size and pH_{pzc} were only evaluated by Brahman et al. [27] for *Tecomella undulata* leaves. The authors reported an average particle size of 66.7 μm and a pH_{pzc} of 4.0, providing insight into the surface charge (positive below pH_{pzc} and negative above pH_{pzc}) behavior of the material as a function of pH.

Applications of Plant Biomass in Rainwater Treatment

Plant biomass has been tested in harvested rainwater treatment for the removal of arsenic and divalent metals. Brahman et al. [27], investigated the removal of arsenic species (As(III) and As(V)) using leaves of *Tecomella undulata* at pH 7.0, with a biosorbent dose of 3.65 g/L and a contact time of 43 min. Under these conditions, removal efficiencies ranged from 71 to 99% for As^{III} and 87–98% for As^{V}. Considering arsenic speciation, As^{III} occurs predominantly as the neutral species H_3AsO_3 up to approximately pH 9, whereas As^{V} is mainly present as $H_2AsO_4^-$ and $HAsO_4^{2-}$ between approximately pH 2–10 [62]. Therefore, the operational conditions applied by Brahman et al. [27] is consistent with the predominant aqueous speciation of both arsenic species, although their adsorption behavior is expected to differ because of their different chemical forms. Ferreira et al. [16] evaluated Zn^{2+} removal using whole beans at pH 5.1–6.4, employing five beans in 50 mL of harvested rainwater. At a contact time of 2 h, Zn^{2+} removal efficiencies ranged from 58 to 85% at 100 μg/L and from 65 to 69% at 500 μg/L. Subsequently, Cabral et al. [26] investigated the simultaneous removal of Zn^{2+}, Cu^{2+}, and Pb^{2+} using bean peels at pH 5.8–6.3, employing one bean peel in 50 mL of harvested rainwater and a contact time of 6 h. Removal efficiencies range from 38 to 83% for Zn^{2+}, 11 to 48% for Cu^{2+}, and 11 to 89% for Pb^{2+} at 100 μg/L, and increase to 32–89%, 23–78%, and 35–97%, respectively, at 500 μg/L. These differences reflect not only variations in contact time and biosorbent configuration, but also differences in experimental systems, as Ferreira et al. [16] evaluated Zn^{2+} in single-metal spiked solutions, whereas Cabral et al. [26] considered multi-metal spiked systems, where competitive interactions may influence sorption behavior.

Cabral et al. [26] further emphasized that, under the near-neutral conditions tested (pH 5.6 and 7.0), the apparent removal of Cu^{2+} and Pb^{2+} may also reflect precipitation rather than adsorption alone. To distinguish adsorption from precipitation, the authors evaluated control systems containing harvested rainwater and mixed metals at pH 4.0, 5.6, and 7.0. Zn^{2+} remained stable throughout the investigated pH range, whereas Cu^{2+}

showed concentration decreases at pH 7.0 and Pb^{2+} from pH 5.6 onwards, consistent with the formation of insoluble hydroxides and carbonates. Based on these observations, the authors concluded that part of the apparent removal of Cu^{2+} and Pb^{2+} under near-neutral conditions could not be exclusively attributed to adsorption. This interpretation is consistent with the recommendations of [57], which proposed that biosorption studies involving divalent metals should preferably be conducted under slightly acidic conditions to minimize precipitation phenomena and ensure that contaminant removal is predominantly governed by adsorption [57].

The proposed use of the rainwater after treatment also differed between studies. Ferreira et al. [16] and Cabral et al. [26] suggested domestic purposes, whereas Brahman et al. [27] proposed its potential use for agricultural irrigation and drinking water production. These findings suggest that biosorbents based on plant biomass can remove arsenic and divalent metals from harvested rainwater. However, the reported removal efficiencies should be interpreted considering solution pH, metal speciation, and the potential occurrence of precipitation, particularly for Cu^{2+} and Pb^{2+}. Careful control of experimental conditions is therefore necessary to distinguish adsorption from other removal pathways.

2.4. Adsorption Mechanisms of Organic and Inorganic Species

Sorption is a broad term that includes both absorption and adsorption [63]. As shown in Figure 3, absorption refers to the uptake of contaminants into the bulk phase of the material, whereas adsorption is limited to interactions occurring at the solid–liquid interface [64]. Adsorption is often the dominant removal pathway because many sorbents provide accessible surface sites for contaminant binding through their surface area, surface chemistry, or a combination of both [29,64,65]. Its efficiency, however, depends not only on the properties of the sorbent but also on the speciation and physicochemical characteristics of the target contaminant [29,65]. Accordingly, mechanistic interpretations must be made on a case-by-case basis, considering both the material and the contaminant involved.

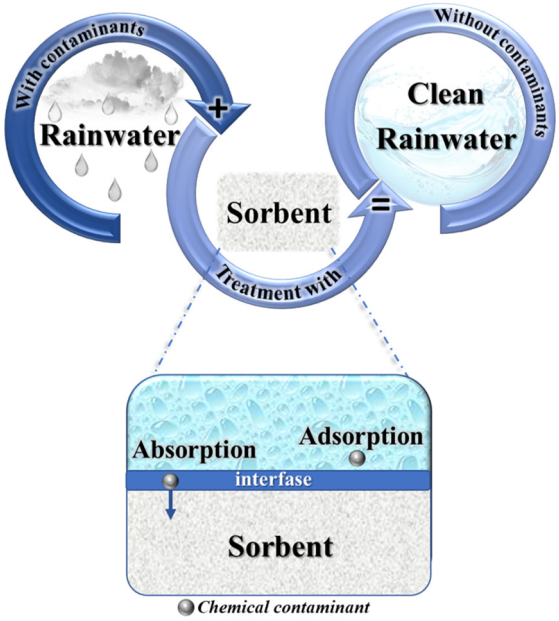


Figure 3. Schematic representation of sorption mechanisms, including adsorption and absorption, at the solid–liquid interface.

Adsorption may occur through physisorption or chemisorption. Physisorption is driven by weak, non-specific interactions such as van der Waals forces and hydrophobic effects, whereas chemisorption commonly involves surface complexation and coordina-

tion, and ion exchange may also contribute depending on the sorbent [66,67]. In practice, both processes may occur simultaneously, and their relative contribution depends on the sorbent surface chemistry, contaminant speciation, pH, ionic strength, and contact time. These general pathways are illustrated in Figure 4a–c, which summarizes the dominant adsorption mechanisms associated with (a) activated carbon, (b) coated sands, and (c) biosorbents based on plant biomass.

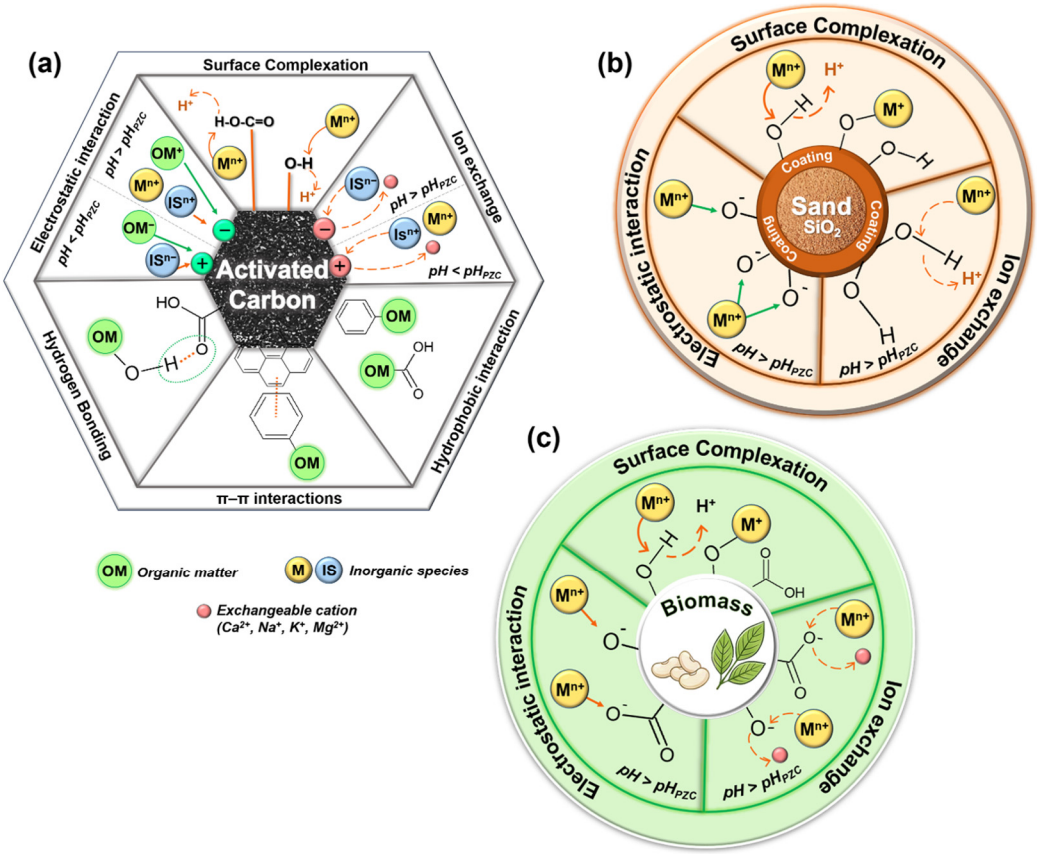


Figure 4. Schematic representation of possible adsorption mechanisms of organic and inorganic species with (**a**) activated carbon, (**b**) coated sands, and (**c**) biosorbent based on plant biomass.

Among the materials used in rainwater treatment, AC has been widely applied for the removal of a broad range of contaminants, including organic matter, potentially toxic elements, and dissolved inorganic ions [23,29,33]. Its highly porous structure and chemically heterogeneous surface allow multiple interactions to occur simultaneously.

As highlighted in Figure 4a, AC commonly contains functional groups such as hydroxyl (-OH), carboxyl (-COOH), and carbonyl (C=O) groups [49]. For organic compounds, adsorption depends on the nature of the organic species in solution and on the functional groups present at the sorbent surface. Hydrophobic interactions promote the adsorption of non-polar organic molecules onto the carbon surface, whereas π–π interactions may further enhance the adsorption of aromatic compounds, and hydrogen bonding may contribute to the adsorption of molecules containing suitable polar functional groups [64,66,68,69]. On the other hand, the adsorption of inorganic species is strongly influenced by solution pH, surface charge, and metal speciation, with surface charge commonly described by pH_{pzc} [70]. Reported pH_{pzc} values for AC vary widely depending on the precursor material and activation method [50]. Therefore, under typical rainwater conditions, which correspond to a pH of approximately 5.6 and are considered chemically neutral for atmospheric waters [3], AC may exhibit a slightly positive, neutral, or slightly negative surface depending on its pH_{pzc}. Therefore, when the pH of the rainwater exceeds the pH_{pzc}, the

AC surface becomes negatively charged and electrostatic attraction of cationic metals is favored. In addition, surface functional groups on the sorbent can coordinate metal ions, and ion exchange may also occur, with protons or naturally associated cations (e.g., Ca^{2+} or Mg^{2+}) being replaced by incoming contaminants [71,72]. At lower pH, competition with protons reduces the availability of these binding sites and weakens metal uptake. Thus, the removal of inorganic species by AC is highly dependent on the relationship between solution pH and surface charge.

Coated sands are typically used as granular supports with reactive surface coatings, most commonly metal oxides or hydroxides, which provide reactive surface sites for dissolved species (Figure 4b). Their removal performance is therefore mainly determined by the properties of the coating surface rather than by the sand core itself. The incorporation of iron and manganese oxides (≡Fe–OH, ≡Mn–OH) provides reactive hydroxylated surface sites capable of binding both cationic and anionic species depending on pH and contaminant speciation [73]. For inorganic species, the dominant mechanisms generally include electrostatic attraction, ion exchange, and surface complexation with hydroxylated coating groups. At higher pH, deprotonation generates negatively charged sites that favor the adsorption of cationic species, although precipitation reactions may also become relevant for metals susceptible to hydrolysis. Moreover, these hydroxylated surface groups can promote the formation of inner-sphere complexes with divalent metal ions through coordination bonds at the oxide coating surface. Ion exchange has also been proposed as a possible contribution to metal retention in iron oxide-based materials. Benjamin et al. [73] described iron oxide-coated sand as an ion-exchange medium, whereas Lo et al. [74] attributed metal uptake primarily to ligand exchange reactions between dissolved metal ions and surface hydroxyl groups, involving the release of H^+ and the formation of stable surface complexes. Furthermore, Cu^{2+} has been shown to undergo strong surface complexation on iron-coated sand, highlighting the importance of specific interactions between metal ions and reactive oxide surfaces [74].

Biosorbents based on plant biomass, shown in Figure 4c, are commonly lignocellulosic materials rich in hydroxyl, carboxyl, phenolic, and, in some cases, amino groups [57]. These functional groups provide multiple binding sites for inorganic species. Plant-derived biosorbents such as white beans (*Phaseolus vulgaris* L.) and their peels function effectively as biosorbents, owing to the polysaccharide-rich structure of their cell walls, naturally enriched in hydroxyl, carboxyl, and amine groups that act as binding sites [16,26]. For inorganic contaminants, the main mechanisms include ion exchange, electrostatic attraction, and complexation with surface functional groups. The main mechanisms involved in metal retention are schematically illustrated in Figure 4c, highlighting how these functional groups interact with cationic metals such as Zn^{2+}, Pb^{2+}, and Cu^{2+}. Ion exchange often predominates, with protons or naturally associated cations such as Ca^{2+}, Mg^{2+}, or K^+ being replaced by incoming metals including Zn^{2+}, Pb^{2+}, and Cu^{2+}. At the same time, deprotonated carboxyl and hydroxyl groups provide negative charges that electrostatically attract cationic metals, while these groups together with amine functionalities can coordinate directly with metal ions to form stable surface complexes. This combination of mechanisms can support efficient metal retention across a range of pH conditions, with acidic environments limiting uptake due to competition from protons, whereas near-neutral pH enhances both electrostatic and coordinative interactions [57]. Spectroscopic studies further confirm the involvement of hydroxyl and carboxyl groups while showing that the structural integrity of the biomass remains largely preserved during sorption [26].

The adsorption of organic and inorganic species from rainwater cannot be explained by a single universal mechanism. The dominant removal mechanism depends on the

physicochemical properties of the contaminant, the composition and pH of the aqueous solution, and the surface characteristics of the sorbent.

2.5. Adsorbent Materials for Rainwater Treatment: Environmental, Economic, and Application Perspectives

The implementation of adsorbent materials for harvested rainwater treatment depends not only on adsorption performance but also on environmental, economic and operational considerations. Table 3 provides a comparative assessment of the main environmental, economic and practical aspects associated with the three adsorbent classes discussed in this review, namely carbon-based materials, surface-modified mineral matrices and biosorbents (based on the studies of Tables 1 and 2). The comparison highlights the characteristics of the three adsorbent classes, demonstrating the versatility of adsorption as a treatment approach for harvested rainwater.

Table 3. Comparative analysis of adsorbent materials for harvested rainwater treatment considering environmental, economic and practical aspects.

Adsorbent Class	Environmental Aspects	Economic Aspects	Full-Scale Applicability	Main Challenges
Carbon-based materials	Biomass-derived materials	Low-cost precursors	Suitable for fixed-bed filters	Performance depending on precursor and activation method
	Waste valorization	Chemical activation increases costs	Suitable for integration into conventional treatment systems	High energy requirements during production
	Regeneration potential	Regeneration may reduce operating costs	Suitable for decentralized treatment systems	Fouling/biofilm formation
	Increased environmental footprint during carbonization and activation		Applicable to both inorganic and organic contaminants	Loss of adsorption capacity after regeneration
Surface-modified mineral matrices	Naturally abundant mineral substrates (e.g., sand)	Mineral substrates are generally inexpensive	Suitable for fixed-bed filters	Performance depending on coating
	Low environmental impact of mineral substrates	Surface modification increases production costs	Suitable for decentralized treatment systems	Coating stability
	Regeneration potential	Regeneration may reduce operating costs	Applicable to inorganic contaminants	Limited long-term field validation
	Increased environmental footprint during surface modification			Evaluated under laboratory conditions
Biosorbents	Biomass-derived materials	Low-cost biomass materials	Suitable for decentralized treatment systems	Performance depending on biomass characteristics
	Biodegradable materials	Locally available materials	Applicable to inorganic contaminants	Potential release of organic matter
	Preparation without chemical modification	Minimal processing requirements	Operational simplicity	Evaluated under laboratory conditions

From an environmental and economic perspective, Table 3 highlights that biomass-derived adsorbents can contribute to resource valorization, while regeneration strategies may reduce material consumption and operating costs. However, adsorbent production

processes, including carbonization, activation and surface modification, may increase both production costs and environmental impacts. Regarding practical applicability, Table 3 shows that carbon-based materials are the only adsorbent class investigated for the removal of both inorganic and organic contaminants, whereas surface-modified mineral matrices and biosorbents have only been evaluated for inorganic contaminant removal, suggesting that adsorption-based systems may also be used for removal of specific contaminants from rainwater. Therefore, the selection of adsorbent material should consider not only removal performance but also sustainability, economic feasibility and operational requirements.

The practical aspects summarized in Table 3 highlight that, although all adsorbent classes have been investigated for harvested rainwater treatment, successful full-scale applications have only been reported for carbon-based materials, particularly activated carbon. These include implementations in residential buildings [22,23], buildings [17,30], university facilities [29], rural schools and health centers [33], and community-scale systems [24,28]. Nevertheless, wider implementation requires further assessment of long-term operational aspects, including maintenance requirements, regeneration efficiency, adsorbent replacement, variability in harvested rainwater quality and the integration of adsorption with complementary treatment barriers to ensure consistent water quality.

The integration of adsorption-based treatment into rainwater harvesting systems represents an important climate adaptation strategy for cities. The safe use of harvested rainwater as an alternative water resource reduces pressure on conventional freshwater supplies while strengthening water resilience under increasing water scarcity and water stress. Moreover, the compatibility of these adsorbent materials with decentralized treatment systems supports adaptive water management in cities, contributing to the development of climate-resilient communities.

3. Final Remarks, Challenges and Future Research

This review highlights that the performance of adsorbent materials for rainwater treatment cannot be interpreted solely from their physicochemical properties. Instead, adsorption behavior results from the interaction between material characteristics, solution chemistry, contaminant speciation, and the occurrence of concurrent removal mechanisms. Evaluating these factors together provides a more consistent explanation of the differences in removal performance reported across the literature and helps explain why similar adsorbent materials often exhibit contrasting results under different rainwater conditions.

This study shows that adsorption may not act as an isolated process when applied to rainwater. Depending on the physicochemical characteristics of both the adsorbent and the water matrix, including pH, contaminant removal may involve simultaneous contributions from adsorption, precipitation, filtration, and biological degradation. Consequently, observed removal efficiencies may overestimate the contribution of adsorption alone when other simultaneous removal mechanisms are not experimentally differentiated. Interpreting adsorption behavior therefore requires considering the physicochemical conditions under which removal occurs rather than evaluating adsorbent properties in isolation.

Despite the increasing number of studies, important challenges remain. Experimental conditions vary considerably, key information on adsorbent properties and solution chemistry is often incomplete, and removal is frequently attributed exclusively to adsorption even when other mechanisms are likely to contribute. These limitations reduce the comparability of the available studies and hinder the establishment of robust relationships between adsorbent characteristics and treatment performance.

Future research should continue exploring new adsorbent materials, particularly those that have not yet been evaluated using real rainwater samples. Expanding the range of materials investigated, however, should be accompanied by experimental designs

that enable meaningful comparisons across studies. A more systematic characterization of adsorbents, together with careful control of solution chemistry and evaluation of concurrent removal mechanisms, will improve the interpretation of adsorption performance and provide a stronger basis for selecting materials according to specific rainwater treatment objectives, intended water uses, and future practical implementation requirements.

Supplementary Materials: The following supporting information can be downloaded at: https://www.mdpi.com/article/10.3390/w18161955/s1, Figure S1: Quantitative assessment of the reviewed literature showing the percentage of the reviewed studies as a function of (a) adsorbent class, (b) contaminant group evaluated for each adsorbent class, and (c) intended post-treatment application of harvested rainwater. Percentages were calculated using the total number of reviewed studies (n = 18; [15–17,19–33]).

Author Contributions: Conceptualization, A.C.D. and P.S.M.S.; methodology, G.T.A.D.S.; validation, G.T.A.D.S., A.C.D. and P.S.M.S.; formal analysis, G.T.A.D.S.; investigation, G.T.A.D.S.; writing—original draft preparation, G.T.A.D.S.; writing—review and editing, G.T.A.D.S., A.C.D. and P.S.M.S.; visualization, G.T.A.D.S.; supervision, A.C.D. and P.S.M.S.; project administration, P.S.M.S.; funding acquisition, A.C.D. and P.S.M.S. All authors have read and agreed to the published version of the manuscript.

Funding: This work was funded by national funds through FCT—Fundação para a Ciência e a Tecnologia I.P., under the project CESAM-Centro de Estudos do Ambiente e do Mar, references UID/50017/2025 (doi.org/10.54499/UID/50017/2025) and LA/P/0094/2020 (doi.org/10.54499/LA/P/0094/2020). G.T.A.D.S. was financially supported by a FCT doctoral grant (SFRH/BD/137755/2018). The research contract of P.S.M.S. was funded by the FCT Scientific Employment Stimulus—Individual 2017 (CEECIND/01835/2017; DOI: 10.54499/CEECIND/01835/2017/CP1459/CT0017).

Data Availability Statement: The original contributions presented in the study are included in the article/Supplementary Materials. Further inquiries can be directed to the corresponding author.

Conflicts of Interest: The authors declare no conflicts of interest.

Abbreviations

AC—Activated Carbon; ACC—Activated Carbon Cloth; ACF—Activated Carbon Fibers; BOD—Biochemical Oxygen Demand; COD—Chemical Oxygen Demand; DO—Dissolved Oxygen; DOC—Dissolved Oxygen Carbon; DOM—Dissolved Organic Matter; EDS—Energy-Dispersive X-Ray Spectroscopy; FTIR—Fourier Transform Infrared Spectroscopy; GAC—Granular activated carbon; IOCS—Iron Hydroxide-Coated Sand; IPCC—Intergovernmental Panel on Climate Change; IUPAC—International Union of Pure and Applied Chemistry; Lab—Laboratory; MOCS—Manganese Oxide-Coated Sand; N.A.—Not Applied; N.R.—Not Reported; OM—Organic Matter; PAC—Powder Activated Carbon; pH_{pzc}—pH Point of Zero Charge; SEM—Scanning Electron Microscopy; SDG—Sustainable Development Goals; TOC—Total Organic Carbon; UV—Ultraviolet; WHO—World Health Organization.

References

1. Biswas, A.; Sarkar, S.; Das, S.; Dutta, S.; Roy Choudhury, M.; Giri, A.; Bera, B.; Bag, K.; Mukherjee, B.; Banerjee, K.; et al. Water scarcity: A global hindrance to sustainable development and agricultural production—A critical review of the impacts and adaptation strategies. *Camb. Prism. Water* **2025**, *3*, e16. [CrossRef]
2. IPCC. *Climate Change 2022: Impacts, Adaptation and Vulnerability. Contribution of Working Group II to the Sixth Assessment Report of the Intergovernmental Panel on Climate Change*; Cambridge University Press: Cambridge, UK; New York, NY, USA, 2022. [CrossRef]
3. Seinfeld, J.H.; Pandis, S.N. *Atmospheric Chemistry and Physics: From Air Pollution to Climate Change*, 2nd ed.; John Wiley & Sons: Hoboken, NJ, USA, 2006.
4. Rathore, S.; Ram, K.; Kumar, P.; Mondal, A. Chemical composition, source apportionment of rainwater, and its contribution to nutrient deposition at an urban site of the middle Indo-Gangetic Plain region. *Atmos. Pollut. Res.* **2025**, *16*, 102518. [CrossRef]
5. Chebbi, A.; Carlier, P. Carboxylic acids in the troposphere, occurrence, sources, and sinks: A review. *Atmos. Environ.* **1996**, *30*, 4233–4249. [CrossRef]

6. Ferreira, M.P.S.; Santos, P.S.M.; Duarte, A.C. Oxidation of small aromatic compounds in rainwater by UV/H_2O_2: Optimization by response surface methodology. *Sci. Total Environ.* **2022**, *815*, 152857. [CrossRef] [PubMed]
7. Santos, G.T.A.D.; Santos, P.S.M.; Duarte, A.C. Vanillic and syringic acids from biomass burning: Behaviour during Fenton-like oxidation in atmospheric aqueous phase and in the absence of light. *J. Hazard. Mater.* **2016**, *313*, 201–208. [CrossRef] [PubMed]
8. Grzegorzek, M.; Wartalska, K.; Szymczewski, S.; Żywiec, J.; Szpak, D.; Kaźmierczak, B. Rainwater quality in Special Economic Zone (SEZ) in Poland. *Environ. Pollut.* **2025**, *370*, 125866. [CrossRef] [PubMed]
9. Bao, H.; Qiao, J.; Huang, D.; Niggemann, J.; Yi, Y.; Zhao, W.; Ni, S.; Dittmar, T.; Kao, S.-J. Molecular level characterization of the biolability of rainwater dissolved organic matter. *Sci. Total Environ.* **2023**, *862*, 160709. [CrossRef] [PubMed]
10. Mitra, S.; Chakraborty, A.J.; Tareq, A.M.; Emran, T.B.; Nainu, F.; Khusro, A.; Idris, A.M.; Khandaker, M.U.; Osman, H.; Alhumaydhi, F.A.; et al. Impact of heavy metals on the environment and human health: Novel therapeutic insights to counter the toxicity. *J. King Saud Univ. Sci.* **2022**, *34*, 101865. [CrossRef]
11. Zhou, X.; Zhou, X.; Wang, C.; Zhou, H. Environmental and human health impacts of volatile organic compounds: A perspective review. *Chemosphere* **2023**, *313*, 137489. [CrossRef] [PubMed]
12. Alkhaldi, H.; Alharthi, S.; Alharthi, S.; AlGhamdi, H.A.; AlZahrani, Y.M.; Mahmoud, S.A.; Amin, L.G.; AlShaalan, N.H.; Boraie, W.E.; Attia, M.S.; et al. Sustainable polymeric adsorbents for adsorption-based water remediation and pathogen deactivation: A review. *RSC Adv.* **2024**, *14*, 33143–33190. [CrossRef] [PubMed]
13. Gkika, D.A.; Tolkou, A.K.; Katsoyiannis, I.A.; Kyzas, G.Z. The adsorption-desorption-regeneration pathway to a circular economy: The role of waste-derived adsorbents on chromium removal. *Sep. Purif. Technol.* **2025**, *368*, 132996. [CrossRef]
14. Dabrowski, A. Adsorption: From theory to practice. *Adv. Colloid Interface Sci.* **2001**, *93*, 135–224. [CrossRef] [PubMed]
15. Ahammed, M.M.; Meera, V. Metal oxide/hydroxide-coated dual-media filter for simultaneous removal of bacteria and heavy metals from natural waters. *J. Hazard. Mater.* **2010**, *181*, 788–793. [CrossRef] [PubMed]
16. Ferreira, M.P.S.; Santos, P.S.M.; Caldeira, M.T.; Estrada, A.C.; da Costa, J.P.; Rocha-Santos, T.; Duarte, A.C. White bean (*Phaseolus vulgaris* L.) as a sorbent for the removal of zinc from rainwater. *Water Res.* **2019**, *162*, 170–179. [CrossRef] [PubMed]
17. Grabowski, T.; Bochniak, A.; Siwiec, T.; Jóźwiakowski, K. Pollutant removal efficiency in a rainwater treatment system in Roztocze National Park (Poland). *Sustainability* **2024**, *16*, 4709. [CrossRef]
18. United Nations. *Transforming Our World: The 2030 Agenda for Sustainable Development*; Resolution A/RES/70/1; United Nations: New York, NY, USA, 2015.
19. Marszałek, A.; Puszczało, E.; Dudziak, M.; Pajdak, A.; Frankowski, J. Evaluation of silkworm cocoon-derived biochar as an adsorbent for the removal of organic and inorganic contaminants from rainwater. *Materials* **2025**, *18*, 5053. [CrossRef] [PubMed]
20. He, J.; Shi, M.; Wang, F.; Duan, Y.; Zhao, T.; Shu, S.; Chu, W. Removal of CX3R-type disinfection by-product precursors from rainwater with conventional drinking water treatment processes. *Water Res.* **2020**, *185*, 116099. [CrossRef] [PubMed]
21. Shaheed, R.; Wan Mohtar, W.H.M.; El-Shafie, A. Ensuring water security by utilizing roof-harvested rainwater and lake water treated with a low-cost integrated adsorption-filtration system. *Water Sci. Eng.* **2017**, *10*, 115–124. [CrossRef]
22. Kus, B.; Kandasamy, J.; Vigneswaran, S.; Shon, H.K.; Moody, G. Gravity driven membrane filtration system to improve the water quality in rainwater tanks. *Water Sci. Technol. Water Supply* **2013**, *13*, 479–485. [CrossRef]
23. Kus, B.; Kandasamy, J.; Vigneswaran, S.; Shon, H.K.; Moody, G. Household rainwater harvesting system: Pilot scale gravity driven membrane-based filtration system. *Water Sci. Technol. Water Supply* **2013**, *13*, 790–797. [CrossRef]
24. Naddeo, V.; Scannapieco, D.; Belgiorno, V. Enhanced drinking water supply through harvested rainwater treatment. *J. Hydrol.* **2013**, *498*, 287–291. [CrossRef]
25. Ahammed, M.M.; Meera, V. Iron hydroxide-coated sand filter for household drinking water from roof-harvested rainwater. *J. Water Supply Res. Technol. AQUA* **2006**, *55*, 493–498. [CrossRef]
26. Cabral, G.H.; Estrada, A.C.; Santos, P.S.M. Removal of Zn(II), Cu(II) and Pb(II) from rainwater by white bean peel: Optimization by response surface methodology. *Appl. Sci.* **2025**, *15*, 627. [CrossRef]
27. Brahman, K.D.; Kazi, T.G.; Afridi, H.I.; Baig, J.A.; Abro, M.I.; Arain, S.S.; Ali, J.; Khan, S. Simultaneously removal of inorganic arsenic species from stored rainwater in arsenic endemic area by leaves of *Tecomella undulata*: A multivariate study. *Environ. Sci. Pollut. Res.* **2016**, *23*, 15149–15163. [CrossRef] [PubMed]
28. Khayan, K.; Husodo, A.H.; Astuti, I.; Sudarmadji, S.; Djohan, T.S. Rainwater as a source of drinking water: Health impacts and rainwater treatment. *J. Environ. Public Health* **2019**, *2019*, 1760950. [CrossRef] [PubMed]
29. Senevirathna, S.; Ramzan, S.; Morgan, J. A sustainable and fully automated process to treat stored rainwater to meet drinking water quality guidelines. *Process Saf. Environ. Prot.* **2019**, *130*, 190–196. [CrossRef]
30. Teixeira, C.A.; Ghisi, E. Comparative analysis of granular and membrane filters for rainwater treatment. *Water* **2019**, *11*, 1004. [CrossRef]
31. Ding, A.; Wang, J.; Lin, D.; Zeng, R.; Yu, S.; Gan, Z.; Ren, N.; Li, G.; Liang, H. Effects of GAC layer on the performance of gravity-driven membrane filtration (GDM) system for rainwater recycling. *Chemosphere* **2018**, *191*, 253–261. [CrossRef] [PubMed]

32. Wu, F.; Li, X.; Tan, Z.; Xue, B.; Wang, Y.; Yan, X. Research on cellar rainwater of northwest region villages and small towns enhanced coagulation by potassium permanganate combined with powdered activated carbon. In Proceedings of the 2012 International Symposium on Geomatics for Integrated Water Resource Management (GIWRM), Lanzhou, China, 19–21 October 2012. [CrossRef]
33. Adler, I.; Hudson-Edwards, K.A.; Campos, L.C. Converting rain into drinking water: Quality issues and technological advances. *Water Sci. Technol. Water Supply* **2011**, *11*, 659–667. [CrossRef]
34. Satyam, S.; Patra, S. Innovations and challenges in adsorption-based wastewater remediation: A comprehensive review. *Heliyon* **2024**, *10*, e29573. [CrossRef] [PubMed]
35. Nasar, A. Carbon-based adsorbents for removing pharmaceuticals from wastewater: A critical review. *JCIS Open* **2026**, *22*, 100175. [CrossRef]
36. Lehmann, J.; Joseph, S. *Biochar for Environmental Management: Science, Technology and Implementation*, 2nd ed.; Routledge: London, UK, 2015.
37. Bansal, R.C.; Goyal, M. *Activated Carbon Adsorption*, 1st ed.; CRC Press: Boca Raton, FL, USA, 2005.
38. Mohan, D.; Sarswat, A.; Ok, Y.S.; Pittman, C.U. Organic and inorganic contaminants removal from water with biochar, a renewable, low cost and sustainable adsorbent—A critical review. *Bioresour. Technol.* **2014**, *160*, 191–202. [CrossRef] [PubMed]
39. Naji, S.Z.; Tye, C.T. A review of the synthesis of activated carbon for biodiesel production: Precursor, preparation, and modification. *Energy Convers. Manag. X* **2022**, *13*, 100152. [CrossRef]
40. Rangabhashiyam, S.; Balasubramanian, P. The potential of lignocellulosic biomass precursors for biochar production: A review. *Ind. Crops Prod.* **2019**, *128*, 405–423. [CrossRef]
41. Cheng, J.; Bi, C.; Zhou, X.; Wu, D.; Wang, D.; Liu, C.; Cao, Z. Preparation of bamboo-based activated carbon via steam activation for efficient methylene blue dye adsorption: Modeling and mechanism studies. *Langmuir* **2023**, *39*, 14119–14129. [CrossRef] [PubMed]
42. Tsai, C.H.; Tsai, W.T. Optimization of physical activation process by CO_2 for activated carbon preparation from Honduras mahogany pod husk. *Materials* **2023**, *16*, 6558. [CrossRef] [PubMed]
43. Mestre, A.S.; Bexiga, A.S.; Proença, M.; Andrade, M.; Pinto, M.L.; Matos, I.; Fonseca, I.M.; Carvalho, A.P. Activated carbons from sisal waste by chemical activation with K_2CO_3: Kinetics of paracetamol and ibuprofen removal from aqueous solution. *Bioresour. Technol.* **2011**, *102*, 8253–8260. [CrossRef] [PubMed]
44. Vargas, D.P.; Giraldo, L.; Moreno-Piraján, J.C. Characterisation of granular activated carbon prepared by activation with $CaCl_2$ by means of gas adsorption and immersion calorimetry. *Adsorption* **2016**, *22*, 717–723. [CrossRef]
45. Zhang, Y.; Song, X.; Xu, Y.; Shen, H.; Kong, X.; Xu, H. Utilization of wheat bran for producing activated carbon with high specific surface area via NaOH activation using industrial furnace. *J. Clean. Prod.* **2019**, *210*, 366–375. [CrossRef]
46. Raval, N.P.; Shah, P.U.; Shah, N.K. Adsorptive removal of nickel(II) ions from aqueous environment: A review. *J. Environ. Manag.* **2016**, *179*, 1–20. [CrossRef] [PubMed]
47. Sing, K.S.W. Reporting physisorption data for gas/solid systems with special reference to the determination of surface area and porosity. *Pure Appl. Chem.* **1982**, *54*, 2201–2218. [CrossRef]
48. Thommes, M.; Kaneko, K.; Neimark, A.V.; Olivier, J.P.; Rodriguez-Reinoso, F.; Rouquerol, J.; Sing, K.S.W. Physisorption of gases, with special reference to the evaluation of surface area and pore size distribution (IUPAC Technical Report). *Pure Appl. Chem.* **2015**, *87*, 1051–1069. [CrossRef]
49. Shafeeyan, M.S.; Daud, W.M.A.W.; Houshmand, A.; Shamiri, A. A review on surface modification of activated carbon for carbon dioxide adsorption. *J. Anal. Appl. Pyrolysis* **2010**, *89*, 143–151. [CrossRef]
50. Kra, D.O.; Allou, N.B.; Atheba, P.; Drogui, P.; Trokourey, A. Preparation and characterization of activated carbon based on wood (*Acacia auriculeaformis*, Côte d'Ivoire). *J. Encapsul. Adsorpt. Sci.* **2019**, *9*, 63–82. [CrossRef]
51. Mailler, R.; Danel, O.; Esperanza, M.; Courtois, S.; Gonzalez Ospina, A. Mastering granular activated carbon filtration to remove organic micropollutants, antibiotic resistance and metals for municipal wastewater reuse. *Sci. Total Environ.* **2024**, *952*, 175918. [CrossRef] [PubMed]
52. Stumm, W.; Morgan, J.J. *Aquatic Chemistry: Chemical Equilibria and Rates in Natural Waters*, 3rd ed.; John Wiley & Sons: Hoboken, NJ, USA, 1995.
53. Areerachakul, N.; Kitiphatmontree, M.; Kandasamy, J.; Kus, B.; Duangduen, C.; Pivsa-Art, S.; Vigneswaran, S. Submerged membrane system with biofilter as a treatment to rainwater. *Water Air Soil Pollut. Focus* **2009**, *9*, 431–438. [CrossRef]
54. Nadagouda, M.N.; Varshney, G.; Varshney, V.; Hejase, C.A. Recent advances in technologies for phosphate removal and recovery: A review. *ACS Environ. Au* **2024**, *4*, 271–291. [CrossRef] [PubMed]
55. Vaishya, R.C.; Gupta, S.K. Coated sand filtration: An emerging technology for water treatment. *J. Water Supply Res. Technol. AQUA* **2003**, *52*, 299–306. [CrossRef]
56. Han, R.; Zou, W.; Zhang, Z.; Shi, J.; Yang, J. Removal of copper(II) and lead(II) from aqueous solution by manganese oxide coated sand. I. Characterization and kinetic study. *J. Hazard. Mater.* **2006**, *137*, 384–395. [CrossRef] [PubMed]

57. Volesky, B. Biosorption and me. *Water Res.* **2007**, *41*, 4017–4029. [CrossRef] [PubMed]
58. Fomina, M.; Gadd, G.M. Biosorption: Current perspectives on concept, definition and application. *Bioresour. Technol.* **2014**, *160*, 3–14. [CrossRef] [PubMed]
59. Park, D.; Yun, Y.S.; Park, J.M. The past, present, and future trends of biosorption. *Biotechnol. Bioprocess Eng.* **2010**, *15*, 86–102. [CrossRef]
60. Michalak, I.; Chojnacka, K.; Witek-Krowiak, A. State of the art for the biosorption process: A review. *Appl. Biochem. Biotechnol.* **2013**, *170*, 1389–1416. [CrossRef] [PubMed]
61. Rashmi, N.; Salmataj, S.A.; Kumar, P.S.; Bhat, P. Exploring chemically and physically modified plant-based fiber biomass for biosorption in wastewater treatment: A concise review. *J. Water Process Eng.* **2024**, *67*, 106245. [CrossRef]
62. Zhang, R.; Wang, L.; Lakho, F.H.; Yang, X.; Depuydt, V.; Igodt, W.; Le, H.Q.; Rousseau, D.P.L.; Van Hulle, S. Iron oxide coated sand (IOS): Scale-up analysis and full-scale application for phosphorus removal from goat farm wastewater. *Sep. Purif. Technol.* **2022**, *284*, 120213. [CrossRef]
63. Ruthven, D.M. *Principles of Adsorption and Adsorption Processes*; Wiley: New York, NY, USA, 1984.
64. Faust, S.D.; Aly, O.M. *Adsorption Processes for Water Treatment*; Butterworth Publishers: Boston, MA, USA, 1988.
65. Rahman, D.Z.; Vijayaraghavan, J.; Thivya, J. A comprehensive review on zinc(II) sequestration from wastewater using various natural/modified low-cost agro-waste sorbents. *Biomass Convers. Biorefin.* **2023**, *13*, 1485–1504. [CrossRef]
66. Israelachvili, J.N. *Intermolecular and Surface Forces*, 3rd ed.; Academic Press: Oxford, UK, 2011.
67. Iakovleva, E.; Sillanpää, M. Novel sorbents from low-cost materials for water treatment. In *Advanced Water Treatment: Adsorption*; Elsevier: Amsterdam, The Netherlands, 2020; pp. 265–359. [CrossRef]
68. Saeidi, N.; Lotteraner, L.; Sigmund, G.; Hofmann, T.; Krauss, M.; Mackenzie, K.; Georgi, A. Towards a better understanding of sorption of persistent and mobile contaminants to activated carbon: Applying data analysis techniques with experimental datasets of limited size. *Water Res.* **2025**, *274*, 123032. [CrossRef] [PubMed]
69. Sigmund, G.; Arp, H.P.H.; Aumeier, B.M.; Bucheli, T.D.; Chefetz, B.; Chen, W.; Droge, S.T.J.; Endo, S.; Escher, B.I.; Hale, S.E.; et al. Sorption and mobility of charged organic compounds: How to confront and overcome limitations in their assessment. *Environ. Sci. Technol.* **2022**, *56*, 4702–4710. [CrossRef] [PubMed]
70. Sen, K.; Mondal, S.; Mondal, N.K. Surface charge behavior of natural and modified adsorbents: Insights into pHzpc, mechanisms, and methodological perspectives. *Next Mater.* **2026**, *11*, 101938. [CrossRef]
71. Robin, V.; Tertre, E.; Beaufort, D.; Regnault, O.; Sardini, P.; Descostes, M. Ion exchange reactions of major inorganic cations (H^+, Na^+, Ca^{2+}, Mg^{2+} and K^+) on beidellite: Experimental results and new thermodynamic database. Toward a better prediction of contaminant mobility in natural environments. *Appl. Geochem.* **2015**, *59*, 74–84. [CrossRef]
72. Yang, X.; Wan, Y.; Zheng, Y.; He, F.; Yue, Z.; Huang, J.; Wang, H.; Ok, Y.S.; Jiang, Y.; Gao, B. Surface functional groups of carbon-based adsorbents and their roles in the removal of heavy metals from aqueous solutions: A critical review. *Chem. Eng. J.* **2019**, *366*, 608–621. [CrossRef] [PubMed]
73. Benjamin, M.M.; Sletten, R.S.; Bailey, R.P.; Bennett, T. Sorption and filtration of metals using iron-oxide-coated sand. *Water Res.* **1996**, *30*, 2609–2620. [CrossRef]
74. Lo, S.L.; Jeng, H.T.; Lai, C.H. Characteristics and adsorption properties of iron-coated sand. *Water Sci. Technol.* **1997**, *35*, 63–70. [CrossRef]

Disclaimer/Publisher's Note: The statements, opinions and data contained in all publications are solely those of the individual author(s) and contributor(s) and not of MDPI and/or the editor(s). MDPI and/or the editor(s) disclaim responsibility for any injury to people or property resulting from any ideas, methods, instructions or products referred to in the content.